An extended travelling fire method framework for performance-based structural design

AN EXTENDED TRAVELLING FIRE METHOD (ETFM) FRAMEWORK FOR PERFORMANCE-BASED STRUCTURAL DESIGN

Xu Dai*[1], Stephen Welch[1], Olivier Vassart[2], Kamila Cábová[3], Liming Jiang[4], Jamie Maclean[1], G. Charles Clifton[5], and Asif Usmani[4]

[1]School of Engineering, BRE Centre for Fire Safety Engineering, Institute for Infrastructure and Environment, The University of Edinburgh, Edinburgh, UK
[2]ArcelorMittal Global R&D, Luxembourg
[3]Department of Steel and Timber Structures, Czech Technical University in Prague, Czech Republic
[4]Department of Building Services Engineering, The Hong Kong Polytechnic University, Hong Kong
[5]Department of Civil & Environmental Engineering, University of Auckland, Auckland, New Zealand

Abstract

This paper presents the extended travelling fire method (ETFM) framework, which considers both energy and mass conservation for the fire design of large compartments. The framework is demonstrated in representing the travelling fire scenario in the Veselí Travelling Fire Test, to identify its capabilities and limitations. The comparison between the framework and the test is achieved through performing a numerical investigation of the thermal response of the structural elements. The framework provides good characterisation of maximum steel temperatures and the relative timing of thermal response curves along the travelling fire trajectory, though it does not currently address non-uniform fire spread rate. The test conditions are then generalised for the purpose of a series of parametric studies which are used to quantify the impact of other design parameters, including member emissivity, convective heat transfer coefficient, total/radiative heat loss fractions, fire spread rate, fire load density and various compartment opening dimension parameters. Within the constraints of this study, the inverse opening factor and total heat loss prove to be the most critical structural fire design parameters. Finally, the ease of using the ETFM framework is illustrated with a sample script using an integrated computational tool, SIFBuilder, based on the OpenSees software framework.

Keywords

travelling fires; performance-based design; structural fire engineering; numerical heat transfer; Veselí Travelling Fire Test; large compartments

1 Introduction

In structural fire design, a key principle is to ensure that the fire resistance of a structure is greater than the fire severity. In order to satisfy this principle quantitatively, rather than qualitatively, three design domains that structural fire engineers can follow are: the time domain, the temperature domain, and the strength domain[1]. Design in the time domain generally refers to the failure time of a structural element under the standard fire, which should be greater than the design fire duration (e.g. one hour, two hours, etc.). Design in the temperature domain normally relates to the maximum temperature in the structural solid under the expected fire, which should be less than the temperature which might induce the structural element to fail. And lastly, design in the strength domain requires the load capacity of the structural element under the fire to be larger than the applied load, to prevent structural failure. By their definitions, it is obvious that these three design domains are interchangeable if the same structural failure criterion is adopted. However, the reliabilities of these respective methods would diminish when different fire exposure models are used to define fire severity. For example, the standard time-temperature curve, e.g. ASTM-E119 fire[2] is adopted for structural fire design in the time domain. It

assumes that all the structural members in the compartment share the same time-temperature histories at any specific time. This may be a reasonable assumption when the compartment size is small. But in the case of vehicles burning in an open car park, which means the fire source is relatively small compared to the whole compartment, localised fire models (e.g. Hasemi localised fire model[3]) are considered to be more appropriate in representing the fire severity for structural fire design. Then, the design in time domain becomes inappropriate compared with the design in the temperature domain, or in the strength domain for this case. Hence this principle would be undermined and difficult to assess with the increasing level of complexity of the structural layout and correspondingly more realistic fire scenarios.

1.1 Why travelling fires

This situation would become even worse when the design compartment is so large that no existing fire exposure model can readily be used by the structural engineers. It implies that even if the design satisfies the strength domain criteria, that will not guarantee its reliability, due to the unknown fire severity paired with the large design compartment. A classic example is the September 11 terrorist attack on the World Trade Center (WTC) buildings in New York City in 2001, where fire is regarded as one of the main reasons that caused the buildings to collapse[4]. The National Institute of Standards and Technology (NIST) reconstructed the fire impact inside of the building compartments using the Fire Dynamics Simulator (FDS) code, to further investigate the collapse of the buildings. One of the key findings is that averaging the gas temperature may lead to large errors in analysing the thermal and structural response, since fire was highly variable in space and was noted to "travel" around the large compartment[5], as shown in Figure 1.

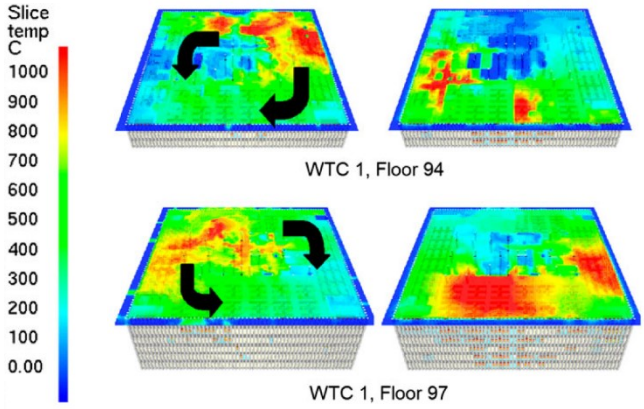

Figure 1. FDS simulated fire movement on floors 94 and 97 of WTC 1, adapted from Gann *et al.*[5].

Apart from the WTC buildings, high temperature inhomogeneity in the large compartments with such developing fire features has been reported several times: the First Interstate Bank Building in Los Angeles in 1988[6], the Windsor Tower in Madrid in 2005[7], and more recently the Plasco Building in Tehran in 2017[8,9]. Furthermore, experimental evidence has also shown high temperature heterogeneity in such compartments and the corresponding threat to the structures. These experiments were reviewed by Stern-Gottfried & Rein in 2012[10], and Dai *et al.* in 2017[11]. These facts underline the urgent need for a better description of fire scenarios for structural design, recognising the trend towards larger spatial layouts preferred in contemporary architecture. One possible solution is performing Computational Fluid Dynamics (CFD) simulations, which can be used to derive the fire severity input for structural design. However, using CFD is typically not feasible on a day-to-day routine design basis for structural engineers, due to the massive computational demands and expert analyst effort it would entail. Moreover, the very detailed outputs that CFD models would generate may become unnecessary or even misleading thermal input information for the structural engineers, as it requires professional fire science knowledge to interpret and judge those results from complex fire scenarios. In addition, outputs may often be highly sensitive to uncertain input parameters. An alternative solution, as proposed here, is to represent these types of fire scenarios by developing a simple design framework, to address the problem in a practical manner, enabling the structural engineers to utilise the concept without resorting to

excessively large computations. An appropriate and efficient level of detail in the model is required to handle these fire scenarios realistically. The work in this paper is developed on this basis.

1.2 Travelling fire methodologies

The problem illustrated above is now being addressed with 'travelling fire' methodologies, which are related to fires that may burn locally and presumed to move across entire floor plates over a period of time in large compartments. There are three explicit representations of travelling fires which can be found in the literature: Clifton's model[12], Rein's model and its subsequent refined versions[13–16], and an extended travelling fire methodology (ETFM) framework *conceptually* put forward by the authors in 2016[17,18]. The ETFM framework is developed by 'mobilising' Hasemi's localized fire model[3] for the fire plume near the structure (i.e. near-field), and combining that with a simple smoke layer calculation by utilising the FIRM zone model[19] for the areas of the compartment away from the fire (i.e. far-field). The temperature field generated by the ETFM framework will enable both a heating phase and a cooling phase for each structural member in the large compartment, schematically presented in Figure 2.

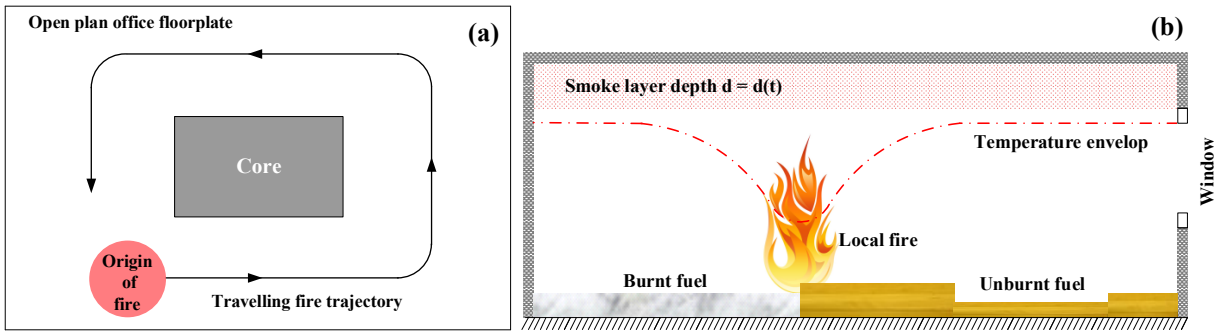

Figure 2. Schematic of the ETFM framework (a) in sectional plan view and (b) in sectional elevation view, adapted from Dai *et al.*[17].

The ETFM framework enables the analysis to capture both spatial and temporal changes of the thermal field. Fire temperatures are variable for the near field, contrasting the uniform 800 °C - 1200 °C assumption in Rein's model, while all elements in one firecell share the same fire exposure history in Clifton's model. Furthermore, the embedded FIRM zone model also enables the ETFM to consider smoke accumulation under the ceiling, which is not explicitly addressed in the other models. More importantly, utilising the FIRM zone model into the ETFM framework means that the energy conservation and the mass conservation are both required to be satisfied for the design compartment. Previously proposed travelling fire methodologies simply force a representation via other existing models to 'travel' (i.e. modified parametric fire curves in Clifton's model, 800 °C – 1200 °C temperature block and the Alpert's ceiling jet model in Rein's model), and have not attempted to explicitly account for the mass and energy balance in the compartment, thus the ETFM framework in principle addresses more of the fire dynamics than the previous models. The work presented in this paper puts forward an easily implementable performance-based design approach for structures with large compartments under travelling fires, through a more fire science-bounded travelling fire model with mass and energy conservation, i.e. the ETFM framework.

1.3 The openings for a design compartment

After more than a decade of research, travelling fires are now regarded as a very relevant fire scenario for large compartments. Typical features of this fire scenario are the fire plume in the near-field and the hot smoke layer providing pre-heating in the far field. Once the fire is "travelling", the near-field has a leading edge representing the fire spread, and a trailing edge representing the burnout of the fuel. Though well understood in concept, the main research efforts on travelling fire methodologies[11] inevitably rely highly on an oversimplified assumption – that travelling fires are mostly fuel-load-driven, i.e. where ventilation plays a very limited role in dictating large compartment design fires.

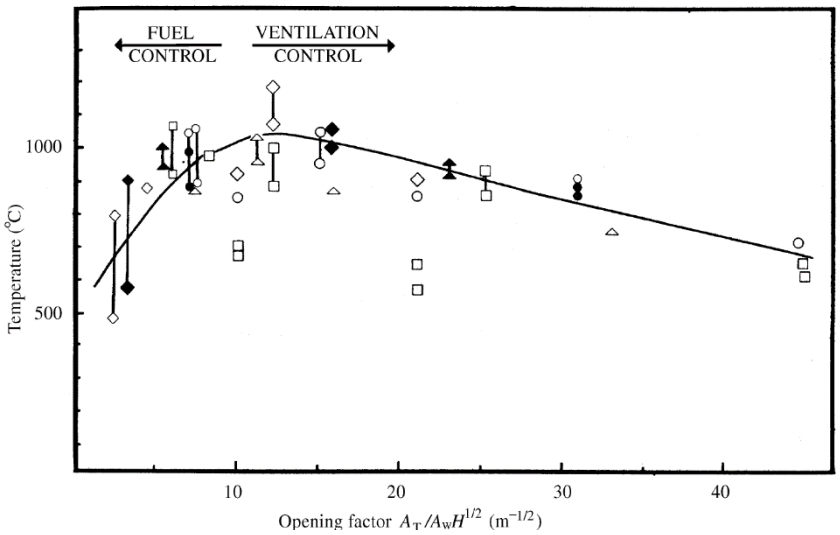

Figure 3. The relationship between the inverse opening factor $A_T/(A_W H^{1/2})$ and the maximum average gas phase temperature in small size compartments, with smallest dimension of 0.5, 1 or 1.5 m (A_T is the total area of enclosure excluding floor and openings area, A_W is the total area of the vertical openings, and H is the weighted average of window heights)[20], original work done by Thomas & Heselden[21].

In literature, this situation is recognised not to hold for small fully engulfed compartments, in which opening factor is one of the dominant variables affecting the maximum average gas phase temperature[20,21], as shown in Figure 3. A value of the inverse opening factor of approximately 10 separates the compartment fire regimes between "fuel-controlled" and "ventilation-controlled", and the maximum temperature decreases in both directions as the inverse opening factor deviates from this value. More recently, Torero *et al.*[22] revisited the conventional compartment fire framework, which is highly relevant to Figure 3 and developed by the pioneers in fire safety engineering (i.e. Kawagoe K., Thomas P.H., and Harmathy T.Z.), concluded that there is in fact no theoretical linkage between the opening factor and the maximum steady state temperature in the compartment for fuel-controlled fires, as historical experimental data shows a high degree of scatter between these two variables. However, they emphasized that the development of the conventional compartment fire framework is generally based upon cubic-like small size (< 150 m^3) compartments. Majdalani *et al.*[23] further explored both the ventilation-controlled fires and fuel-controlled fires experimentally and numerically, with a 0.82 m wide, 0.82 m high, and 1.06 m deep test compartment. Via extrapolation from these results it was suggested that fuel-controlled fires are more practical and perhaps more critical for structural fire design in large compartments compared with ventilation-controlled fires. Via a test series in large compartments (5 m wide, 2 m high, and 18 m deep) Maluk *et al.*[24] quantitatively challenged the validity of the conventional compartment fire framework, through analysing the energy distribution under different ventilation conditions[25]. This energy distribution analysis showed that the largest contribution of the energy loss is through compartment openings. This finding implies that considering fuel-controlled fires with large openings in a design compartment would generally underestimate the fire impact for structural design compared to ventilation control, and the importance of the openings, and uncertainties in glazing failure, for a large design compartment under travelling fires should be addressed. This implication fits the observation and analysis of the NIST report for the First Interstate Bank Building fire[6], which was a high-rise building fire occurring in 1988 in Los Angeles, US, with large open-plan office areas (approx. 1394 m^2 on each floor). It was observed that the fire started at the southeast corner of the 12th floor, and spread both horizontally and vertically to the upper floors (13th - 15th floors and part of the 16th floor), and lasted for about two hours. It was found that both the fire damage level and spread rate on the 12th floor were higher at the fire initiation area when the ventilation was limited, compared with the opposite side of the building on the 12th floor when the ventilation was improved due to the increasing number of window breakage as the fire developed and propagated.

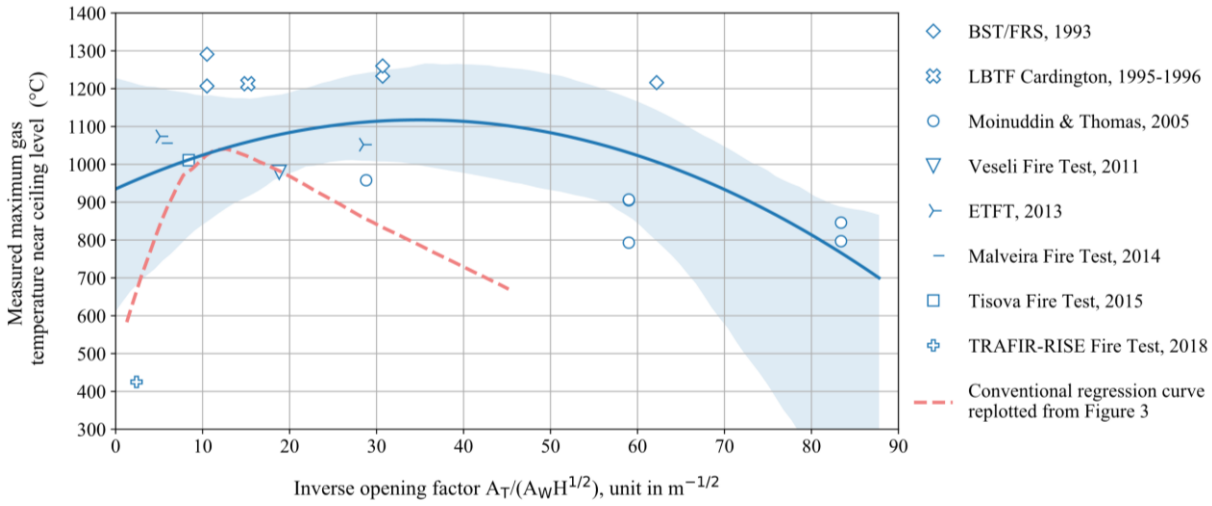

Figure 4. The relationship between the inverse opening factor $A_T/(A_w H^{1/2})$ and the measured maximum average gas phase temperature $T_{g,max}$ near ceiling level of test large compartments, through reviewing previous large-scale natural fire tests with a clear travelling fire development, performed in the past three decades. (solid curve in blue is the 2nd order polynomial regression line for all the reviewed travelling fire tests, and dashed red curve is the same curve presented in Figure 3 for small size compartments as a reference; the translucent blue band describes a bootstrap confidence interval of the estimated regression line according to the available data sampling points).

Figure 4 reviews the previous full-scale natural fire tests carried out in large compartments, where a clear travelling fire development had been identified or targeted, for investigating the relationship between the inverse opening factor $A_T/(A_w H^{1/2})$ and the maximum average gas phase temperature $T_{g,max}$ near ceiling level. Though the reviewed tests adopt various fire load densities, it is still important to note that the research target is the same, i.e. open-plan office buildings. The reviewed full-scale travelling fire experiments include: the British Steel Technical (BST)/Fire Research Station (FRS) 1993 fire test series[26], the Building Research Establishment (BRE) test at Cardington Large Building Test Facility (LBTF) in 1995-1996 for Test 6 (Simulated Office)[27], the Moinuddin & Thomas fire test series[28] in 2005, the Veselí Travelling Fire Test[29] in 2011, the Edinburgh Tall Building Fire Tests (ETFT)[25,30] for test number 11 and 12 using wood sticks in 2013, the Malveira Fire Test[31] in 2014, the Tisova Fire Test[32] in 2015, and the TRAFIR-RISE Fire Test in 2018. The detailed test set-up of these travelling fire experiments has been reviewed by the authors in the previous work[11], except for the Malveira Fire Test and TRAFIR-RISE Fire Test which are so far unpublished. It is also worth noting that a potentially very relevant travelling fire test of the St. Lawrence Burns Project[33] is not included in the review work here due to the limited access of the test data.

In general, Figure 4 illustrates that conditions in the majority of the travelling fire tests for large compartments lie in the traditional ventilation-controlled regime (i.e. the inverse opening factor is greater than 10). However, the regression curve presented in Figure 4 suggests that the regime 'division number' shifts from about 10 for small compartments to closer to 30 for the large compartments reviewed here. When the inverse opening factor is larger than 30, it is apparent that $T_{g,max}$ decreases when the inverse opening factor increases (i.e. smaller openings are adopted) in the large design compartment. This trend is supported by the Moinuddin & Thomas 2005 test series, if we look at closely at this single systematic test series. The main reason for this trend is apparent when considering that, in ventilation-controlled fires, as the opening size decreases oxygen starvation may take place, thereby affecting the combustion efficiency and bringing down the average gas phase compartment temperature. Furthermore, the relationship between the inverse opening factor and the $T_{g,max}$ is not very clear for the travelling fire tests with inverse opening factors less than 30, let alone less than 10. It only shows a weak dependence of the relationship, suggesting that the $T_{g,max}$ gradually decreases while the inverse opening factor is reduced. This dependence of the relationship is less obvious compared with the small-size compartments under fuel-controlled regime, as presented with a dashed red curve in Figure 4.

Based upon the above discussions, especially for the observations from the First Interstate Bank

Building fire[6], the energy distribution analysis by Maluk *et al.*[24], and the regression curve for identifying the relationship between the inverse opening factor and $T_{g,max}$ through reviewing the large scale travelling fire experiments in Figure 4, it can be seen that the opening conditions for a design large compartment might still be a useful design parameter in the travelling fire methodologies for performance-based structural design.

1.4 Research objectives

An extended travelling fire method (ETFM) framework is presented considering both the energy conservation and mass conservation for the design large compartment, for the purpose of assessing whether the structure is able to resist more realistic fire exposures expected in such compartments, for performance-based structural design. Some of the initial ETFM applications were presented in Dai *et al*. (2017)[11]. It is worth noting that those parametric studies were performed by running the 'travelling Hasemi' component and FIRM zone model component separately, to investigate the individual, rather than combined, thermal impacts.

The aims of the current work are to (1) present the full version of the ETFM framework with relevant design instructions which can be readily used by the structural fire engineers; (2) apply the ETFM framework to represent a travelling fire scenario in a real building, i.e. the Veselí Travelling Fire Test building, to further assess the capabilities and limitations of the framework; and (3) perform design parameter sensitivity studies, and parametric studies on the ETFM framework, with the same Veselí Test Building case, in order to interpret the importance of different design parameters (e.g. the inverse opening factor) for travelling fires.

2 ETFM Framework

2.1 Near field: Hasemi's localized fire model

For quantifying the local effect of the travelling fire on adjacent structural members, Hasemi's localized fire model[3] is utilized in the ETFM framework. This correlation model was originally developed with a series of laboratory scale fire tests[34–37] in Japan, with maximum heat release rate (HRR) up to 900 kW. Then, additional validation tests of this model were conducted in Europe with fire size from 2 MW to 60 MW, for both large compartments and car parks[38]. Franssen *et al*.[39] put forward three correlation equations which provide the external heat flux received at the level of the ceiling. These correlations were eventually adopted in Eurocode 1 as the "localized fire model"[40]: when the fire plume is impinging the ceiling, the external heat flux, $\dot{h}$ (W/m^2), is given as:

$$\begin{aligned} \dot{h} &= 100000 && \text{if} && y \le 0.30 \\ \dot{h} &= 136300 - 121000y && \text{if} && 0.30 < y \le 1.0 \\ \dot{h} &= 15000y^{-3.7} && \text{if} && y \ge 1.0 \end{aligned} \quad (1)$$

The parameter y is obtained using the following equation:

$$y = \frac{r + H + z'}{L_h + H + z'} \quad (2)$$

where r (m) is the horizontal distance between the vertical axis of the fire and the point along the ceiling in which the heat flux is calculated, H (m) is the distance between the fire source and the ceiling, L_h (m) is the horizontal flame length (see Figure 5):

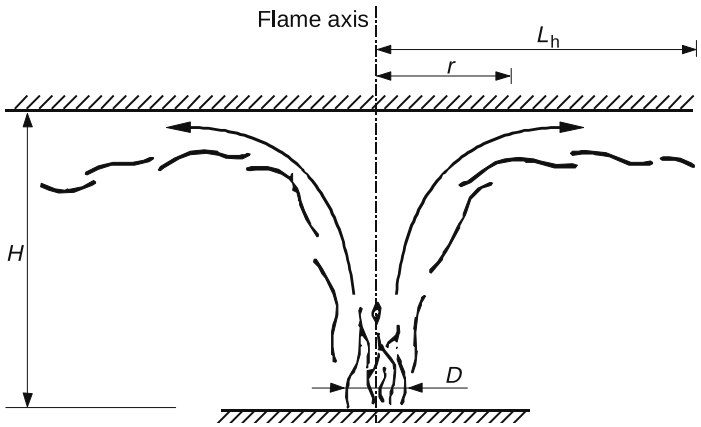

Figure 5. Hasemi's localized fire model in Eurocode 1[40].

L_h (m) is given by the following relation:

$$L_h = (2.9H(Q_H^*)^{0.33}) - H \tag{3}$$

with Q_H^* a non-dimensional HRR given by:

$$Q_H^* = \dot{Q}/(1.11 \times 10^6 \times H^{2.5}) \tag{4}$$

z' (m) is the vertical distance between the virtual fire origin and the fire source, which is given by:

$$\begin{aligned} z' &= 2.4D\left(Q_D^{*\,2/5} - Q_D^{*\,2/3}\right) && \text{if} \quad Q_D^* < 1.0 \\ z' &= 2.4D\left(1.0 - Q_D^{*\,2/5}\right) && \text{if} \quad Q_D^* \geq 1.0 \end{aligned} \tag{5}$$

where $Q_D^* = \dot{Q}/(1.11 \times 10^6 \times D^{2.5})$, D (m) is the diameter of the fire, $\dot{Q}$ (W) is the HRR of the localised fire. Hence, to employ Hasemi's localized fire model into the ETFM framework, three key parameters should be determined transiently: the location of the fire, the evolving fire diameter, D (m), and HRR, $\dot{Q}$ (W), because they are each constantly changing when fire 'travels' in the compartment. Details of how these parameters are approximated according to the features of the travelling fire is illustrated in the following several sections.

2.2 Far field: FIRM zone model

In most practical buildings, smoke will probably accumulate under the ceiling if its movement is interrupted, due to the walls or smoke protection soffits which are built around the ceiling edges. Therefore, the smoke accumulation is brought into the ETFM framework through utilising a zone model in an elementary way. The depth of the smoke layer is time-dependent and uniformly distributed over the whole ceiling (as illustrated in Figure 6). This feature is capable of reproducing pre-heating and post-heating effects for the structural design. There are several zone models available in the literature, with two popular ones being OZone[41,42] and CFAST[43]. However, the ETFM framework employs the FIRM zone model[19] for its smoke layer calculation. The main reason is that FIRM is relatively simple and easy to implement, which matches the ethos of the ETFM framework. At the same time FIRM possesses all the basic components that a zone model should have: fire source, smoke plume, air entrainment, hot upper layer, cold lower layer, smoke flow through vents, and heat losses through thermal boundaries (i.e. walls, ceilings), and the most fundamental: mass conservation and energy conservation. Moreover, FIRM was the first fire model which was fully documented, validated, verified, and evaluated following the ASTM guidelines back in 2000[19,44].

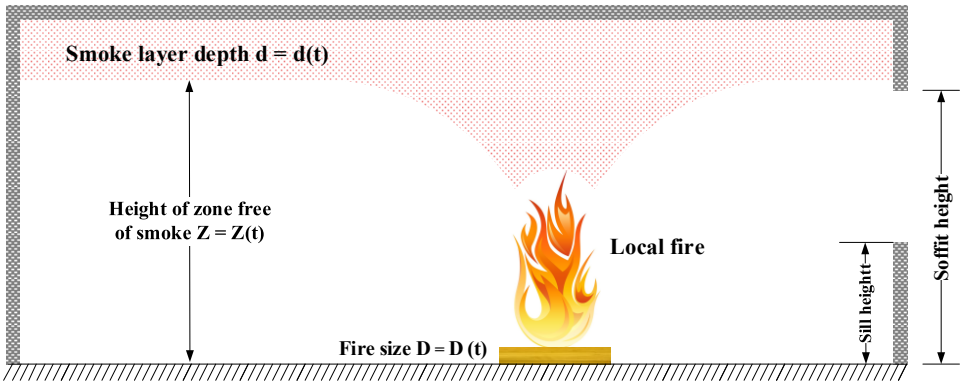

Figure 6. Schematic of the smoke for far field in the ETFM framework.

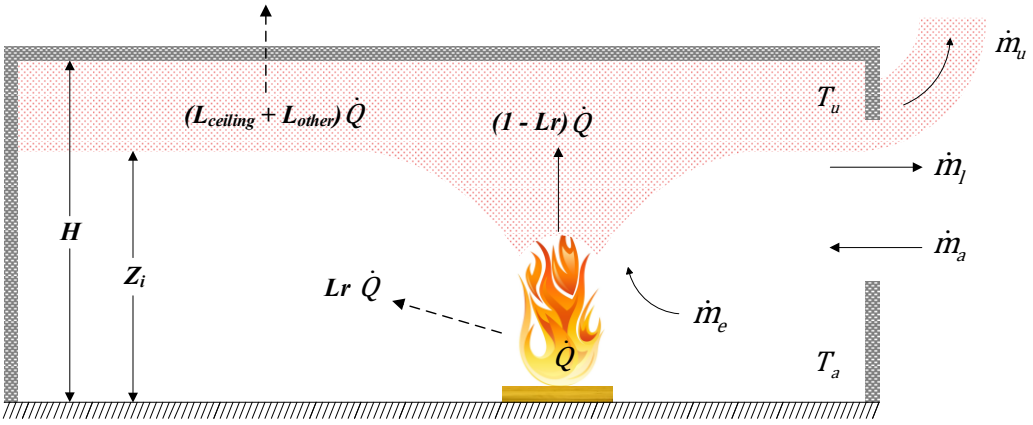

Figure 7. Schematic of the mass conservation and energy conservation of the FIRM zone model in ETFM.

Two time-varying outputs are represented through the FIRM zone model, i.e. the transient upper smoke layer temperature, T_u (K), and the evolution of the smoke layer interface height, Z_i (m). The determination of these two variables is achieved via solving a set of ordinary differential equations (ODEs) based on mass and energy conservation, such as the mass conservation of the lower ambient air to obtain transient Z_i[19]:

$$\frac{dZ_i}{dt} = \frac{\dot{m}_a - \dot{m}_l - \dot{m}_e}{\rho_a A} \tag{6}$$

where t (s) is the time, $\dot{m}_a$ (kg/s) is the vent flow rate of the ambient air entering the compartment (an upper limit $(\dot{m}_a)_{max} = 0.52 A_v \sqrt{H_v}$ is setup for ventilation-controlled burning while oxygen is limited, in which A_v is the area of the vertical opening, H_v is the clear opening height), $\dot{m}_l$ (kg/s) is the lower layer vent flow rate leaving the compartment, $\dot{m}_e$ (kg/s) is the air entrainment mass flow rate, $\rho_a = 1.2$ kg/m^3 is the density of the ambient air, and A (m^2) is the total compartment area, see Figure 7.

Figure 7 schematically illustrates the mass and energy balance of the design compartment. In addition to the mass balance in this figure, $\dot{m}_u$ (kg/s) is the smoke vent flow rate leaving the compartment, and H (m) is the clear height of the compartment. Another key ODE concerns the upper smoke layer energy conservation to obtain the transient upper layer temperature, T_u[19]:

$$\frac{dT_u}{dt} = \frac{T_u\left[(1 - L_c)\dot{Q} - \dot{m}_e c_p (T_u - T_a)\right]}{c_p \rho_a T_a A (H - Z_i)} \tag{7}$$

where $\dot{Q}$ (kW) is the HRR of the fire, $T_a = 294.26$ K is the ambient air temperature, $c_p = 1.004$ kJ/kg·K is the assumed constant specific heat, and L_c is the assumed constant total heat loss fraction ratio (0.6 ~ 0.9 as recommended in Janssens[19], in general, 0.6 refers to well-insulated compartment

thermal boundaries, and 0.9 refers to poorly-insulated compartment thermal boundaries).

In addition, L_r is the radiative loss fraction of the fire plume (0.15 ~ 0.40 as recommended in Janssens[19]). The relationship between L_c and L_r is explained in Eqn. 8, where the total heat loss fraction L_c consists of $L_{ceiling}$ (the fraction of heat losses in the form of ceiling convection), L_r, and L_{other} (heat losses fraction due to the roughness of ceilings or aspect ratio of the compartment, suggested to vary from 0 for very smooth ceilings or high aspect ratio compartments, to 0.3 for very rough ceilings or low aspect ratio compartments[19]).

$$L_c = L_r + L_{ceiling} + L_{other} \tag{8}$$

In the ETFM framework, only L_c and L_r need to be specified, hence $L_{ceiling} + L_{other}$ can be obtained as a lumped value. It is worth noting that L_c and L_r are both empirical values but very fundamental to the resultant smoke layer temperature calculations. Figure 7 also schematically illustrates the energy balance of the design compartment. Typically, a part of the total HRR of fire, $L_r\dot{Q}$, is radiated away from the combustion region, and the rest $(1 - L_r)\dot{Q}$ is convected up through the plume into the formation of the upper hot smoke layer. A fraction of this energy $(L_{ceiling} + L_{other})\dot{Q}$ is assumed to be lost from the smoke layer to the compartment boundaries through convection and radiation. Then the remaining energy at the upper layer, $(1 - L_c)\dot{Q}$, would directly contribute to the gas temperature of the smoke, i.e. the sensible enthalpy. It is important to note that another main source of energy loss is through the openings. This is accounted for by the format of mass loss from the hot smoke layer venting, and explicitly calculated by the mass balance calculation for the entire compartment, which is given as:

$$\dot{m}_u T_u - \dot{m}_e(T_u - T_a) - \rho_a T_a A \frac{H - Z_i}{T_u}\frac{dT_u}{dt} + (\dot{m}_a - \dot{m}_l)T_a = 0 \tag{9}$$

In addition, there may be no significant differences in terms of smoke temperature rises by using different air entrainment models[45]. Two air entrainment models can be selected in the ETFM framework: the Thomas model[46], which is widely used in the UK for venting calculations[20]:

$$\dot{m}_e = 0.188 W_{fi}(Z_i)^{3/2} \tag{10}$$

where W_{fi} (m) is the perimeter of the fire, or Zukoski's model[47], which is given as:

$$\dot{m}_e = K(1 - L_r)^{1/3}\dot{Q}^{1/3}(\Delta Z_i)^{5/3} \tag{11}$$

where $K = 0.076$, ΔZ_i is the distance between the fuel top surface and the smoke layer interface. In the ETFM framework, the thickness of the fuel is ignored, hence $\Delta Z_i = Z_i$.

2.3 Combination of the near field and the far field

Since Hasemi's equation is applicable to localized fires in an unconfined space and smoke accumulation is not considered in his model, this may lead to the far field predicted gas temperature based on Hasemi's localized fire calculation in a confined space being lower than the actual temperature. Therefore, it is proposed here to combine Hasemi's model with a hot smoke layer calculation (i.e. the FIRM zone model) in the ETFM framework. It is then assumed that the radiant and convective heat fluxes to structural surfaces can be calculated based on the *summation* of heat flux from Hasemi's localized fire model and the heat flux from the FIRM zone model (see Figure 8). The proposed way of combining two models may sometimes be over-conservative in adding heat fluxes from two models in the overlap zone where both have a significant value, and in reality there would be some interaction. However, this is considered to represent a relatively small amount of uncertainty in the general complexity of the overall travelling fire framework for the structural design, and is conservative. A "consistent level of crudeness" should be maintained all through our predictions for the structural fire performance problems[48]. Conducting one part of the analysis with very accurate data (e.g. fire model analysis), with an out of balance level of accuracy for another part of the same analysis (e.g. thermo-mechanical

analysis) is inefficient. By contrast, another way of combining a localised fire model with a zone model can also be found in a European research project called "Development of design rules for steel structures subjected to natural fires in large compartments"[49]. This project aimed to update the Eurocode for the design of steel structures with large compartments under the natural fire safety concept. It was proposed that taking the highest temperature along the length of the beam which was predicted by the Hasemi's localized fire model, or the zone model, rather than the heat flux superposition from the two models as proposed here for ETFM.

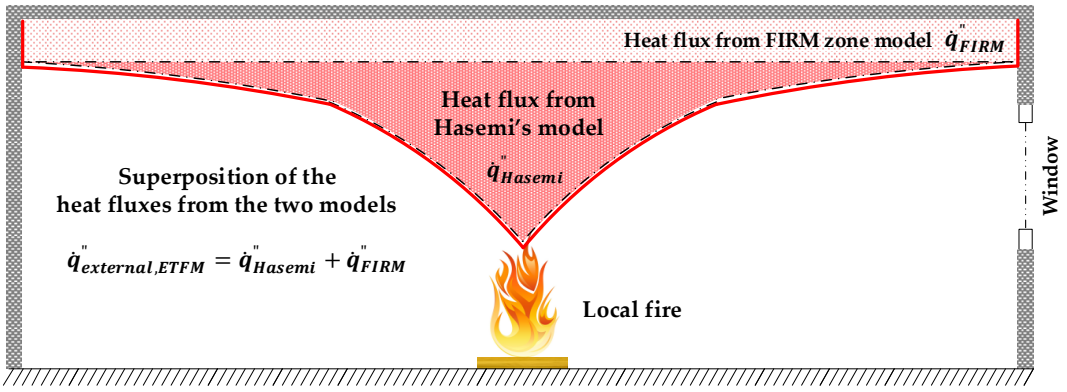

Figure 8. Heat fluxes 'combination' of the two models, i.e. Hasemi localised fire and FIRM zone model.

2.4 Heat release rate (HRR) $\dot{Q}$

Table 1. Maximum RHR_f depending on occupancies, adapted from Eurocode 1[40].

Maximum heat release rate per unit area RHR_f

Occupancy	RHR_f (kW/m²)	Occupancy	RHR_f (kW/m²)	Occupancy	RHR_f (kW/m²)
Dwelling	250	Classroom of a school	250	Office	250
Hospital (room)	250	Shopping centre	250	Theatre (cinema)	500
Hotel (room)	250	Transport (public space)	250	Library	500

The two most important parameters in the ETFM framework are the travelling fire speed which determines how long the "mobile" Hasemi localized fire will affect the structural element involved in the localised burning; and its total HRR, $\dot{Q}$, which determines how efficiently the thermal energy will be released due to the fire plume. The total HRR, $\dot{Q}$, discussed in this section is to be used for Eqns. 4 and 5 to implement Hasemi's localized fire model, and Eqns. 7 and 11 to implement the FIRM zone model, both transiently. Although in Eurocode 1 the expression for calculating HRR, $\dot{Q}$, during the fire growth phase (t-squared fire evolution) is specified[40], the development phase of the travelling localized fire is not considered significant from the structural design point of view. Due to the above reason, and for retaining the simplicity of the ETFM framework, the total HRR, $\dot{Q}$(W), is given by the following expression according to Eurocode 1:

$$\dot{Q} = 1000 \times RHR_f \times A_{fi} \tag{12}$$

where A_{fi} (m²) is the burning area of the fuel, RHR_f (kW/m²) is the maximum HRR per unit area. The determination of RHR_f for different occupancies can be referred to Eurocode 1, which is shown in Table 1. Since RHR_f is a value corresponding to the stationary state of the fire, it implies that the fire in the ETFM framework is actually a "localised fully engulfed" fire which covers a certain burning area

of the fuel (i.e. A_{fi}), and travels on the floor plate as time evolves. Furthermore, the entrainment-controlled burning is considered in FIRM[19], which means the upper bound values are assumed for the air mass flow rate, $\dot{m}_e$, and corresponding HRR, $\dot{Q}$. Assuming Zukoski's plume model is employed, $\dot{m}_e$ and $\dot{Q}$ are changed to:

$$(\dot{m}_e)_{max} = 55K^{3/2}(1 - L_r)^{1/2}(\Delta Z_i)^{5/2} \quad (13)$$

$$(\dot{Q})_{max} = 3030(\dot{m}_e)_{max} \quad (14)$$

As this ETFM framework is basically a localized fire travelling along a predefined trajectory, i.e. one-dimensional, the burning area of fuel A_{fi} is determined by three variables: the travelling fire leading edge derived from the assumed constant fire spread rate, v (mm/s), the travelling fire trailing edge derived from the burn-out time, t_b (s), and the compartment width derived from the floor plan dimensions. Figure 9 illustrates how the burning area of fuel, A_{fi} (m^2), is obtained schematically.

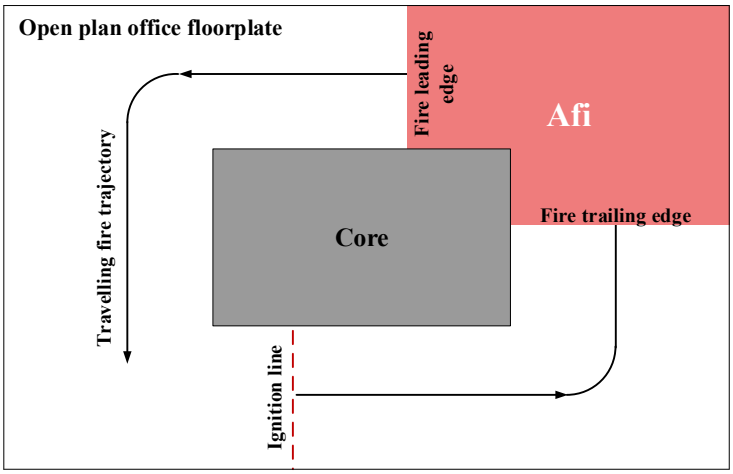

Figure 9. The determination of burning area of fuel A_{fi}.

2.5 Speed of the travelling fire

Table 2. Fire spread rate v from experiments and real fire observations.

Data sources	Fire spread rate v (mm/s)	Data sources	Fire spread rate v (mm/s)
Edinburgh Tall Building Fire Tests (ETFT)[25,30]	1 - 20	Reconstruction of WTC fires	2.5 – 16.7
Tisova Fire Test[32]	0.33-0.67	St. Lawrence Burns tests	7.5 - 13
Natural Fires in Large Scale Compartments" tests[26]	1.5 - 19.3	First Interstate Bank fire	14.5

Fire spread rates will vary hugely depending on the circumstances, thus for design exercise a range will normally be specified; in defining representative numbers some have analysed real fires (Rackauskaite *et al.*[16] cites 14.5 mm/s for the First Interstate Bank fire and 2.5-16.7 mm/s for WTC fire reconstructions), travelling fire tests (Rackauskaite *et al.*[16] cite 1.5-19.3 mm/s for Kirby *et al.* "Natural Fires in Large Scale Compartments" tests[26] and 7.5-13 mm/s for the St. Lawrence Burns tests, to which can be added 0.33-0.67 mm/s initial spread rate in the Tisova Fire Test[32] and 1 mm/s at the start of the ETFT timber crib tests rising to c. 20 mm/s in the main fire spread period from 30-35 minutes. Clifton adopted rates of 8.3 mm/s for low opening factors (<0.06) and twice that for higher ones. Comparing with other design methods, it is noted that inversion of the assumed fire growth rates, e.g. those given in the Eurocode 1, gives 3.3 mm/s for 'slow', up to 13.3 mm/s for 'fast' fire growth rates, respectively.

2.6 Burn-out time t_b

Table 3. Characteristic fuel load densities $q_{f,k}$ depending on occupancies, adapted from Eurocode 1[40].

Characteristic fuel load densities $q_{f,k}$ (average)					
Occupancy	**$q_{f,k}$ (MJ/m²)**	**Occupancy**	**$q_{f,k}$ (MJ/m²)**	**Occupancy**	**$q_{f,k}$ (MJ/m²)**
Dwelling	780	Classroom of a school	285	Transport (public space)	100
Hospital (room)	230	Shopping centre	600	Office	420
Hotel (room)	310	Theatre (cinema)	300	Library	1500

In this ETFM framework it is assumed that all fuel would be consumed over the entire fire duration. Therefore, to determine the travelling fire trailing edge location, a burn-out time, t_b (s), is introduced. t_b is a similar variable assumed in Rein's travelling fire model[16] for quantifying the time needed for burning out a certain area of fuel completely. It is obtained by the following equation:

$$t_b = 1000 \times q_{f,k}/RHR_f \tag{15}$$

where $q_{f,k}$ (MJ/m²) is the characteristic fuel load density. The reference values of $q_{f,k}$ for different occupancies can be referred to Eurocode1[40], which is adapted into Table 3. Figure 10 schematically illustrates how the burning area of fuel A_{fi} is determined with the burn-out time t_b concept.

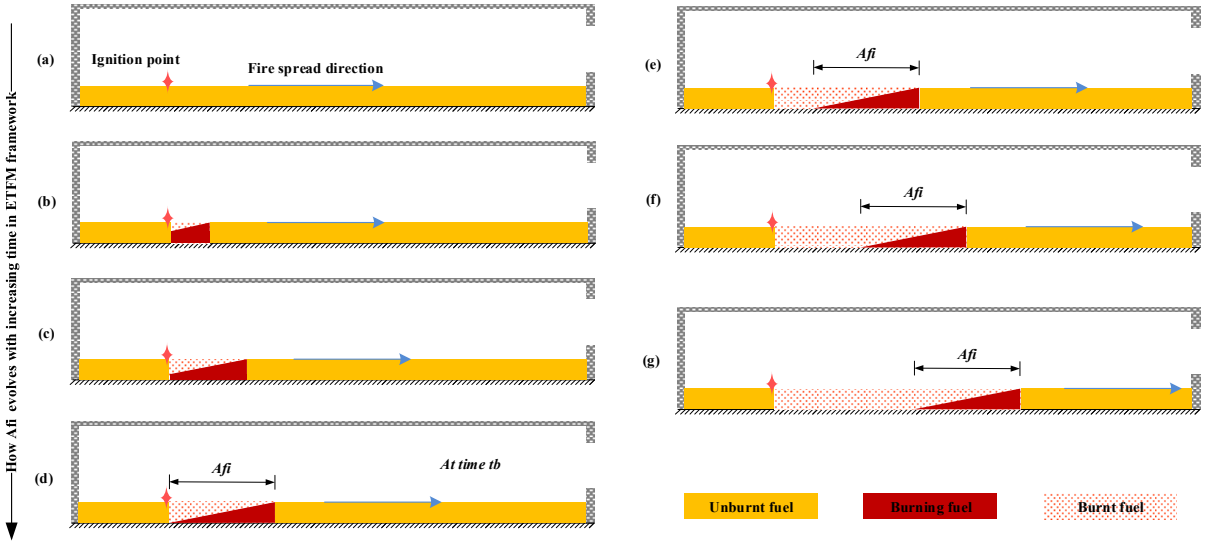

Figure 10. Determination of burning area A_{fi} with burn-out time t_b concept – in elevation view, (a) to (g) with a certain time sequence.

2.7 Approximation of Fire Location and Fire Diameter *D*

Once the burning area of fuel A_{fi} is determined, the fire location of the travelling Hasemi's localized fire model can be obtained, which is defined as the centre of the distance between the travelling fire leading edge and trailing edge along the trajectory. Furthermore, the fire diameter D (m) of the travelling Hasemi's localized fire can be approximated as the diameter of a circular source of the same burning area of fuel A_{fi} (m²), which is given by:

$$D = 2\sqrt{A_{fi}/\pi} \tag{16}$$

2.8 Other key assumptions

As the final objective of this ETFM framework is for its application to structural design, the travelling fire trajectory is assumed to be under the mid-span of the main beams (see Figure 2 (a)), which would normally represent the worst case for the structural response.

A concept of "regulatory minimum fuel depth" (RMFD) is introduced into the ETFM framework, corresponding to a reference travelling fire spread rate, v (see Table 2), and a certain level of fuel load density, $q_{f,k}$ (see Table 3). This RMFD is a layer of fuel uniformly distributed over the entire floor plate, and contributes to the total heat flux calculation. The unburnt fuel in Figure 10 is an RMFD.

The ETFM framework considers both the fuel-controlled and ventilation-controlled conditions, with the assumption that sufficient air is available at the beginning and subsequently the glazing adjacent to the main fire region breaks. This is likely to happen in many fires considering window glazing failure at 150 °C – 200 °C[50]. Then the analysis may step into the entrainment-controlled burning or the ventilation-controlled burning, depending on the transient status of the air entrainment mass flow rate, $\dot{m}_e$, and the ambient air inflow rate through the compartment openings, $\dot{m}_a$, respectively.

A flashover scenario arises naturally in this model, and the fire transits from a localized travelling fire to a whole compartment fire when a defined threshold is met, e.g. the temperature of the hot smoke layer reaches 600 °C. It is noted that for determining when flashover occurs in the compartment there are three commonly-used indicators[20]: 1) the temperature of the smoke in the whole compartment reaches 600 °C; 2) heat fluxes produced from the fire are as high as 20 kW/m^2 at the floor level; 3) for ventilation-controlled fires, significant flaming emerges from the window(s). Each of these definitions is a very crude indicator of the flashover state, and for simplicity clause 1) is adopted in the current ETFM framework.

2.9 Implementation of the ETFM framework

To facilitate the ETFM framework as an easy-to-use design tool for the structural fire engineers it is implemented into an OpenSees-based[51], open-source software framework called SIFBuilder[18,52,53] using C++. SIFBuilder integrates the analysis of fire, heat transfer and thermo-mechanical response of the structure in one single software package. Due to limited space, the detailed implementation and verification of the ETFM framework is not presented in this paper but can be found in the first author's PhD thesis[53]. SIFBuilder is used with the ETFM framework to perform both the fire and heat transfer analysis in the subsequent sections of this paper.

Figure 11. Experimental building during the Veselí Travelling Fire Test.

3 Application of the ETFM Framework for the Veselí Travelling Fire Test Building

Performance-based design for structures in fire requires validated methodologies. Validation of fire spread predictions is very ambitious, nevertheless, in literature it is apparent that none of the travelling fire design methods have been rigorously compared against any real travelling fire experiments so far[11]. This section demonstrates the application of ETFM framework to representation of fire spread in a real building, i.e. the Veselí Travelling Fire Test building[29] (a two-storey steel-composite structure, as shown in Figure 11). It is achieved through performing a numerical investigation of the thermal response of the structural elements, i.e. comparing member temperatures between the predicted time-temperature histories using the ETFM framework and the test data. The efforts of this comparison demonstrate the capability of the ETFM framework, and further identify some of its limitations.

3.1 Veselí Travelling Fire Test (Czech Republic, 2011)

In 2001, a travelling fire test was conducted on the upper floor of a two-storey steel composite building in Veselí, Czech Republic, as part of a collaborative project funded by Research Fund for Coal and Steel (RFCS) in the European Commission, called COMPFIRE[54]. The test aimed to investigate how a travelling fire might impact the structural components, especially for beam-to-column connections. It suggested that the travelling fire should be taken into account as one of the worst-case fire scenarios, since the cyclic heating and cooling due to the fire movement would cause cyclic deflections of the structural members, and this type of fire scenario is not considered in traditional structural fire design where it is assumed that homogeneous temperatures pertain in the whole compartment[29].

The dimensions of the test building were 13.4 m long × 10.4 m wide × 9 m high, with a 5 m × 2 m unglazed opening on each floor to provide enough ventilation for a smooth development of the fire[55], as presented in Figure 12. The test compartment internal size was 12 m × 9 m. The test compartment was well-insulated[55], as linear trays K 120/600/0.75 mm + mineral wool Rockwool 120 mm in depth with density 40 kg/m^3 + trapezoidal sheet TR 35/207/0.63 mm were used as the wall linings, and 100 mm depth steel-composite slabs were used as the ceiling with lightweight concrete C30/37 + steel S350 trapezoidal sheets Cofraplus 60 with thickness 0.75 mm. The fuel bed was continuous in a 'band strip' shape (8 m × 3 m), using wood sticks (50 mm × 50 mm × 1000 mm per stick) as the fuel load. Every square metre of fuel bed consists of 6 layers of 7 wood sticks, approximately to fuel load density of 47.25 kg/m^2 (i.e. equivalent to 680 MJ/m^2 if assuming the chemical heat of combustion of the wood sticks[56] to 18 MJ/kg with combustion efficiency[57] 0.8), as shown in Figure 13.

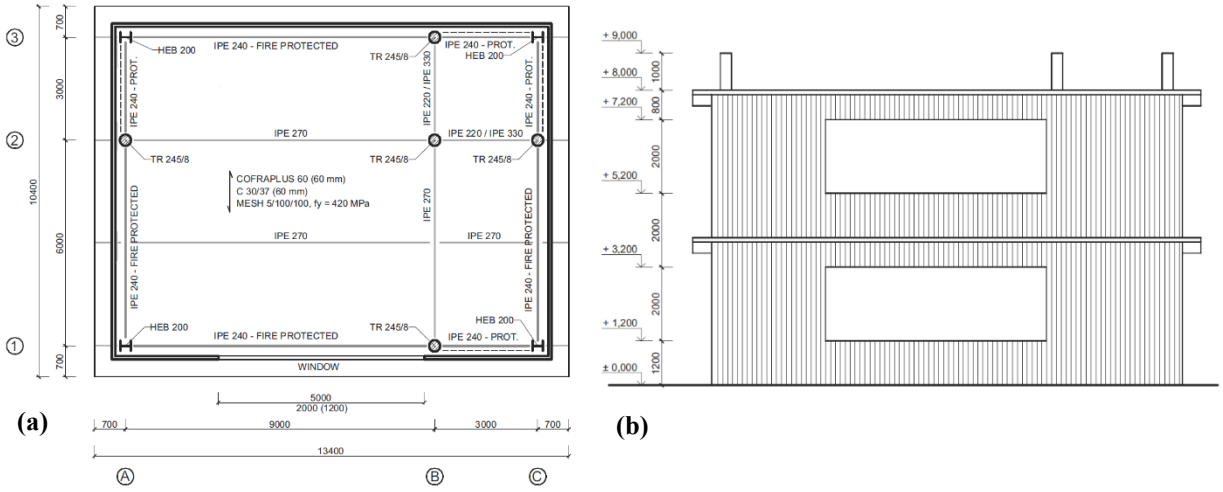

Figure 12. Veselí test building in (a) plan-view with approximate clear floor area 12 m × 9 m, and (b) in elevation view with one side vertical opening 5 m × 2 m on the test upper floor (dimensional unit in plots is mm), from Wald *et al.* [55].

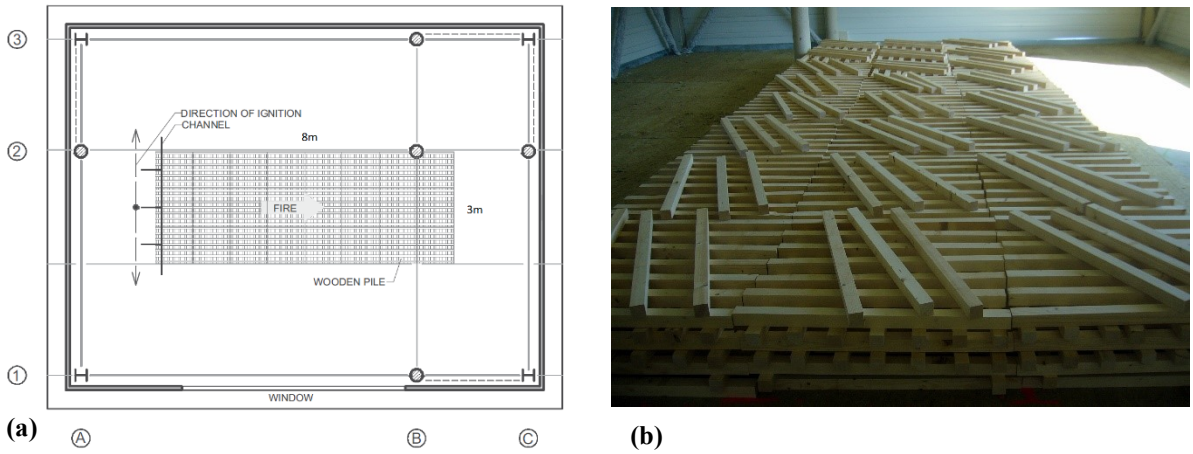

Figure 13. Veselí Travelling Fire Test fuel load scheme (a) in hatched 8 m × 3 m, on the upper floor of the experimental building[55], and (b) front view with wood stick size 50 mm × 50 mm × 1000 mm, with 6 layers of 7 sticks per square meter, approximate to fuel load density 680 MJ/m^2 within the hatched fuel bed.

Figure 14. Fire development in the Veselí Travelling Fire Test[11].

The fire was ignited with a linear source at one end of the fuel bed to allow the fire free to develop. Figure 14 demonstrates the fire development at every 5 mins during the test. Three phases of the fire can be identified, including: Phase I from 0 to 15 mins, while the fire leading edge was gradually spreading over the majority of the fuel bed and a clear smoke layer accumulation was observed; Phase II from 20 to 25 mins, while a 'quasi' flashover happened during this short time period, but no external flames coming out of the opening were noted (as noted, the latter being one of the classical criteria for defining a conventional flashover fire); Phase III from 30 to 40 mins, the fire trailing edge continued moving to the other end of the fuel bed, accompanied by a clear decaying of the fire. Thus, this travelling fire was partially fuel-controlled when the fire was spreading and decaying during Phase I and Phase III, and partially influenced by the ventilation when the smoke accumulation occurred during Phase I and 'quasi' flashover during Phase II.

Figure 15(a) presents the well-instrumented test compartment[55], including gas phase temperature via thermocouple (TG series), plate thermometer temperature (PT series), radiant heat flux (R series), beam temperature (TB series), connection temperature (TC series), slab temperature (TS series), and column temperature (TSG series). Furthermore, unlike other travelling fire tests, the structural response during the fire development was also recorded, including the vertical and horizontal displacement of the slab (V and H series, respectively), the deflection of the beam mid-span (V series), and the strain gauge on the columns (SG series). Nevertheless, it is worth noting that the crib weight loss was not measured, which means it is not easy to characterise the evolving heat release of the fire.

3.2 Preparation for the 'comparison' – heat transfer validation for SIFBuilder

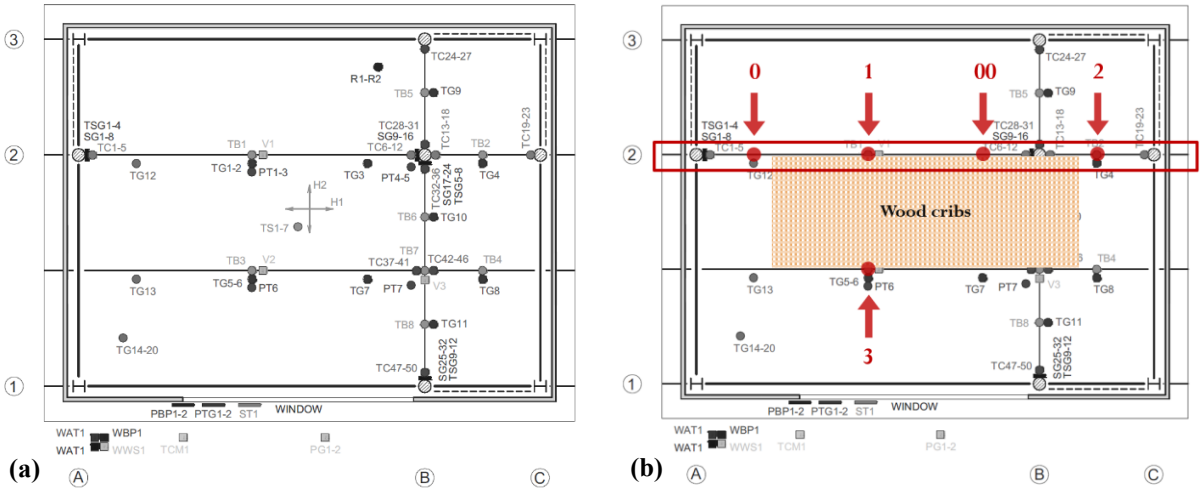

Figure 15. (a) Instrumentations at the test compartment ceiling level[55], details of these instrumentation symbols can be found in the main text, and (b) investigated TG (gas phase temperature via thermocouple) and TB (beam temperature) locations for the ETFM framework comparison with the test data (marked in red dots, with tags 0 - TG12, 1 - TB1 & TG2, 00 - TG3, and 2 - TB2 & TG4; 3 - TB3 & TG6 is for the SIFBuilder heat transfer validation only), fuel bed distribution in hatched.

In order to compare the predictions from the ETFM framework with the Veselí Travelling Fire Test, locations near ceiling level (i.e. the bottom flange of the steel beams) with tags 0, 1, 00, 2 are selected for investigation, as shown in Figure 15(b). The reason for selecting this series of locations is because those points are in parallel with the travelling fire trajectory, and relatively far away from the openings, to minimise the wind-induced test data uncertainty. Furthermore, considering that the ETFM framework essentially generates heat fluxes as the thermal boundaries for the subsequent heat transfer analysis, and all four investigated locations 0, 1, 00, 2 have gas phase temperature measurement via thermocouple (TC) at the vicinity of the lower flange of the steel beams (with corresponding tags TG12, TG2, TG3 and TG4 respectively), it is not straightforward to compare the heat flux from the ETFM framework with the measured TC temperatures from the test. Alternatively, temperatures at the bottom flange of the steel beams may be chosen as the targeted variable for comparison, which requires heat transfer analysis using the heat flux from the ETFM framework, and TC temperatures from the test as the thermal boundaries, respectively.

SIFBuilder is used to perform the proposed heat transfer analysis for comparison. As mentioned in Section 2.9, it is an integrated numerical tool based on several OpenSees-related thermal modules, in which the heat transfer module was originally developed, and extensively verified as well as validated, by Jiang[58]. Nevertheless, the validity of applying the heat transfer module for the conditions of the Veselí Travelling Fire Test still needs to be quantified, and if it is necessary, the built-up heat transfer model may require to be further calibrated with the test data for the subsequent comparison. In addition, due to the limited availability of the measured bottom flange steel temperatures at the investigation locations (only TB1 at location 1 and TB2 at location 2 are available, but TB1 failed after 15 mins during the test), another location with tag 3, having measurements TB3 and TG6, is introduced as an additional heat transfer validation point, as shown in Figure 15(b).

Figure 16 indicates the credibility of SIFBuilder heat transfer module, through comparing the measured steel beam bottom flange temperatures, TB2 and TB3, with the SIFBuilder heat transfer results, which use the corresponding lower flange TC temperatures in the vicinity, TG4 and TG6 respectively. The measured TG4 and TG6 are applied as the thermal boundaries on three sides of the investigated steel beam IPE270, excluding the top of the beam where a steel-composite slab is located. Two dimensional heat transfer analysis is carried out for the cross-section, using the convection coefficient, $h_c = 35$ W/m^2 K as 'natural fire' for the fire-exposed surfaces, and emissivity of the steel, $\varepsilon_m = 0.7$ (two values

as recommended in the Eurocode[40]). Figure 16(a) shows that SIFBuilder heat transfer results at TB2 are slightly higher than the measured TB2, by about 10%, when the maximum temperature reaches to 782 °C and 714 °C, respectively. In addition, the SIFBuilder results at TB2 reach the maximum temperature at 29.1 mins, which is about 3.6 mins delayed compared with the corresponding measured value of 25.5 mins. Moreover, Figure 16(b) demonstrates that the SIFBuilder heat transfer results at TB3 agree well with the measured TB3, in terms of the maximum temperatures, 727 °C and 748 °C, respectively, and that the SIFBuilder prediction is around 3% less than the measured value. Further, the timing of reaching the maximum temperatures from SIFBuilder and the measured values is very close, i.e., both at around 25 mins. It is important to note that there are possible uncertainties for the above validations, partially because in reality both the h_c and ε_m, are changing according to the fire development and the steel beam heating process, respectively, however in the work here these two values are assumed to be constant, in accordance with the Eurocode, partially because the adopted input thermal boundaries for heat transfer are the TC temperatures, which are not the actual gas temperatures. As suggested through the work by Welch *et al.*[59], using TC temperature as heat transfer input should not always be seen as a significant disadvantage while the fire is localised or 'travelling', as TC temperature may be dominated by radiation, which can be regarded as a better characteristic of the thermal exposure than gas temperature. The true gas temperature is only equivalent in well-mixed sooty hot layers, which don't fit our case here, i.e., the Veselí Travelling Fire Test.

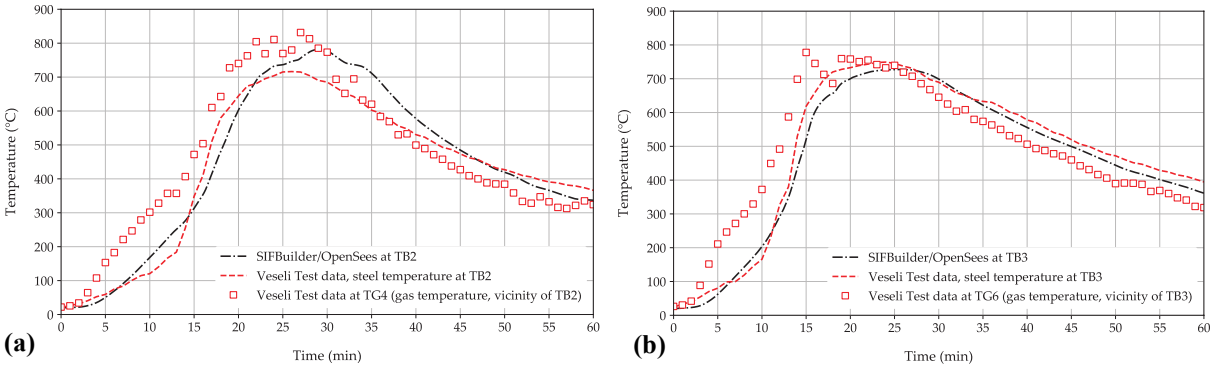

Figure 16. Heat transfer (HT) results from SIFBuilder at the bottom flange of the steel beams IPE270, at (a) TB2 at location 2 using TC temperature TG4 as HT input, and at (b) TB3 at location 3 using TC temperature TG6 as HT input, to compare the measured steel beam bottom flange temperatures with the SIFBuilder HT results.

3.3 ETFM framework vs. Veselí Travelling Fire Test (VTFT)

Figure 17(a) quantitatively confirms the three phases of fire development identified in section 3.1 during the VTFT. At Phase I (0 - 15 mins), measured TC temperatures at locations 0, 1, 00 and 2 are all increasing due to the spreading of the fire leading edge. Meanwhile, a clear 'time difference' is also found among the four time-temperature curves, mainly due to the relative locations of those measured TCs along the fire trajectory. To be more specific, during the initial 5 mins the TC temperature histories at locations 0, 1 and 00 are very close to each other when the fire started, and TC temperature at location 2 is relatively lower, as it is far from the current burning fuel bed. From 5 to 15 mins the above trend is clearer, even among the TC temperature histories at locations 0, 1 and 00. At 15 mins, the results show that TG2 at location 1 reaches as high as 885 °C, due to the direct fire exposure right beneath this location; TG12 at location 0 reaches 726 °C, which is slightly higher than TG3 at location 00, which reaches 643 °C, when the fire travels away from location 0 and into the direction of location 00. After the flashover transition from 15 to 20 mins, at Phase II (20 - 25 mins) all TCs reach their maximum temperatures, where TG2 and TG3 both reach around 950 °C and TG12 and TG4 around 800 °C. This maximum temperature difference between the centre of the compartment (location 1 and 00) and the edge of the compartment (location 0 and 2), again, challenges the conventional post-flashover compartment fire models with an assumed uniform temperature distribution (e.g. standard fire, or parametric fire curves). After 25 mins, including Phase III (30 - 40 mins), measured TC temperatures at locations 0, 1, 00 and 2 are all decreasing due to the movement of the fire trailing edge (i.e. the decay

of the fire). This is different from Phase I where a clear 'time difference' was identified among those time-temperature curves as the fire spread along the fire trajectory; in contrast, all the time-temperature histories 'converge' to a very similar cooling trend here, from 30 mins to 60 mins. This suggests that the cooling stage is not mainly driven by the decaying of the burning fuel, as no 'time-difference' is identified, but is mainly due to the compartment characteristics, such as the thermal boundaries.

Figure 17(b) presents the heat transfer results from SIFBuilder at the bottom flange of the steel beams using the corresponding measured TC temperatures as heat transfer boundary conditions, at locations 0, 1, 00 and 2. It is worth noting that locations 0, 1 and 00 are at the vicinity of steel member IPE270, while location 2 is at vicinity of steel member IPE220, see Figure 12(a). The convection coefficient, $h_c = 35$ W/m^{2}K and emissivity of the steel, $\varepsilon_m = 0.7$, are adopted, according to the work done in section 3.2. In addition, Figure 17(b) shows a very similar heating and cool sequence among those four time-temperature histories at the bottom flanges, compared with what is presented in Figure 17(a).

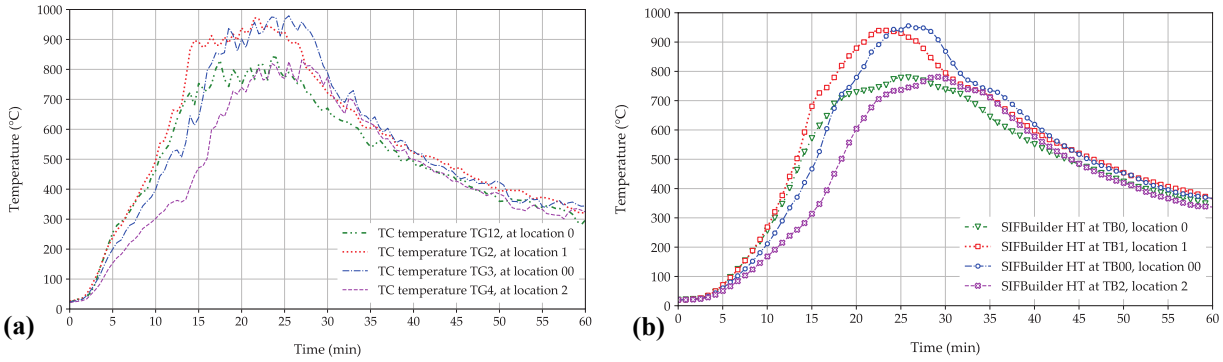

Figure 17. Temperature development along fire trajectory in the test at locations 0, 1, 00 and 2, through representing (a) measured thermocouple (TC) temperatures at the vicinity of the lower flange of the steel beams, and (b) heat transfer (HT) results from SIFBuilder at the bottom flange of the steel beams using the measured TC temperatures shown in (a) as HT input boundary conditions (same colours for curves in (a) & (b) if at corresponding same locations).

```
38   # FIRE DEFINITION
39   AddFire -floor 1 -type ETFM_Travelling_Fire -IgnitionLine point1 2 4 3 point2 2 4 6
     -fireTravelDirection AntiClockWise;
40
41   # MORE FIRE INFO
42   AddFirePars -floor 1 -type ETFM_Travelling_Fire -combination 1 1 -plumeModel Zukoski
     -totalHeatLossFraction 0.68 -radiativeHeatLossFraction 0.25 -ventWidth 5 -sillHeight
     1.2 -soffitHeight 3.2;
43
44   # FUEL LOAD DISTRIBUTION DEFINITION
45   AddFuel -RMFD 1 -Floor 1 -RefinedDimension point1 2 4 3 point2 2 4 6 point3 10 4 6
     point4 10 4 3 -SpreadRate 6.5 -FuelLoadDensity 680 -HRRperArea 700;
```

Figure 18. Corresponding fire part of the model script in Tcl, using the ETFM framework in SIFBuilder for VTFT (Tool Command Language[62], abbrev. Tcl, is a high-level, string-based, scripting language).

As demonstrated in Figure 18, to achieve the comparison between the ETFM framework and VTFT, it is worth noting that the selected input parameters for the ETFM framework have three sources: 1) the exact test setup information, including compartment dimension 12 m × 9 m, fuel load distribution shape 8 m × 3 m, opening size 5 m × 2 m, opening location (i.e. sill height 1.2 m), and fire ignition location; 2) estimated values based on the relevant VTFT publications, including total heat loss fraction 0.68 according to the thermal lining information from the test[55], fuel load density 680 MJ/m^2 with an assumed chemical heat of combustion of the wood sticks[56] to 18 MJ/kg with combustion efficiency[57] 0.8, fire spread rate 6.5 mm/s based on test observations, and maximum HRR per unit area according to Horová *et al.*[56]; 3) empirical values/formulas, e.g. Zukoski's plume model[47], and radiative heat loss fraction 0.25 as recommended in Janssens[19]. During the process of selecting appropriate parameters for the EFTM framework, it is very important to clarify that, both source 2) and source 3) would introduce a certain level of modelling uncertainties. Such uncertainties are unavoidable, so it is of great importance to perform a certain level of fire modelling calibration with the test and subsequent parameter sensitivity

studies, rather than to directly proceed to the "validation" of the fire model, as suggested by Torero *et al.*[60]. Two parameters are adjusted for the calibration, one is the fire spread rate 6.5 mm/s, and the other is the total heat loss fraction ratio 0.68. According to the test observation, the fire spread rate was accelerating throughout Phase I (0 - 15 mins), see Figure 14. A rough estimate of the uniform fire spread is 3, 5.8 and 8.9 mm/s, corresponding to fire spreads to positions at 0.9, 3.5 and 8 m, at 5, 10 and 15 mins, respectively. Due to the steady spread velocity assumption of the current version of ETFM framework, a constant value of 6.5mm/s is adopted. Accompanying with further calibration using total heat loss fraction, $L_c = 0.68$, a reasonable comparison between the ETFM framework and the VTFT is found. Though it may vary with time in practice, the value of $L_c = 0.68$ lies within the general range of 0.6 ~ 0.9 as recommended by Janssens[19], where generally 0.6 refers to well-insulated compartment thermal boundaries, and 0.9 refers to poorly-insulated compartment thermal boundaries. In VTFT, 120mm mineral wool Rockwool was used which will therefore tend to be more towards the well-insulated condition.

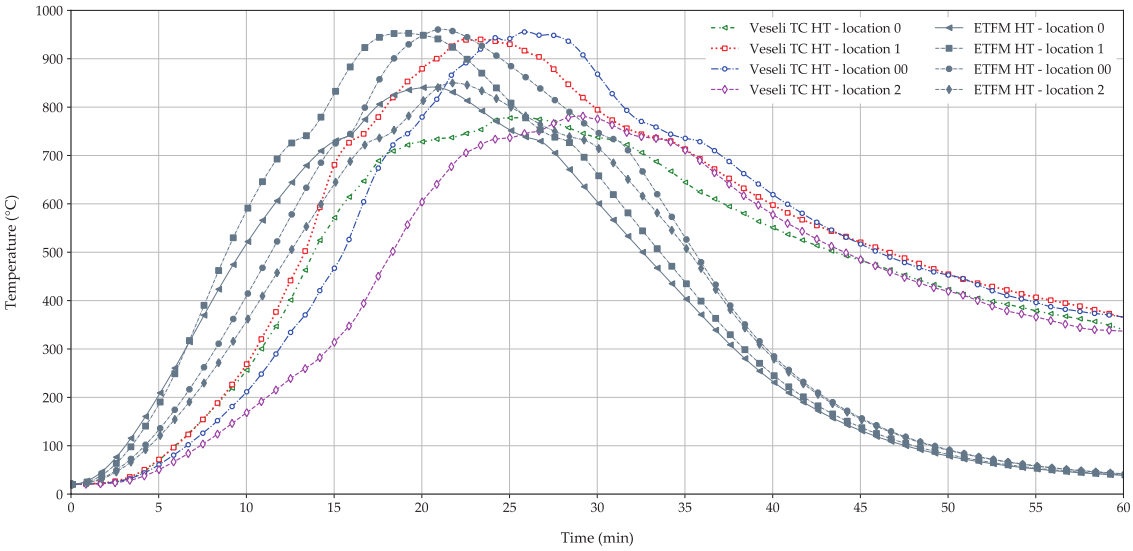

Figure 19. Comparison between the ETFM framework and the Veselí Test, using steel temperatures at bottom flanges, at locations 0, 1, 00 and 2 respectively in the fire spread direction (Veselí thermocouple (TC) temperatures at the vicinity of beam bottom flanges are used as input for SIFBuilder heat transfer (HT)).

Figure 19 demonstrates the comparison through quantifying beam member bottom flange temperatures at various locations along the fire trajectory, between the predicted time-temperature histories using the ETFM framework (model input parameters shown in Figure 18) and the calculated time-temperature histories using the test TC data as heat transfer input. It suggests a good agreement between the ETFM framework and the VTFT, in terms of maximum steel temperatures at various locations along the fire trajectory. Since a constant fire spread rate of 6.5 mm/s is used in the ETFM framework, in contrast to the accelerating fire spread of 3 to 8.9 mm/s as observed in the test, a clear 'offset' of results between the framework and the test can be identified. To 'filter out' this offset due to the ETFM framework assumption of using a constant fire spread rate, all time-temperature history predictions from the framework presented in Figure 19 were applied with a 4 mins time shift, as shown in Figure 20(a).

Figure 20(b), (c), (d), and (e) present the time-shifted comparison using the beam member bottom flange temperatures between the ETFM framework and the VTFT at location 0, 1, 00 and 2 respectively. Those four figures mostly suggest that the ETFM framework can generate good predictions during the heating stage of the travelling fire at various locations along the fire trajectory, except the location 2, which is at the opposite side of the fire ignition location. This suggests that the uniform temperature assumption due to the pre-heating of the smoke upper layer from the FIRM zone model of the ETFM framework may over-predict the temperature at the far-field. However, this overprediction is not of great concern because it generates more conservative temperature for a design fire. More importantly, a large discrepancy is found at all four locations during the decaying stage of the travelling fire. This discrepancy is undesirable as it implies that the predicted time-temperatures from the ETFM framework

will be far lower than the test results. A possible reason in using the ETFM framework along with SIFBuilder is that as soon as the fire is decaying and even diminishing, the resultant heat release rate (HRR) will decrease drastically. This HRR determines the efficiency of the energy 'pumped up' to the upper smoke layer, which highly affects the resultant design fire temperatures. However, in reality (i.e. during the test) the temperature during the cooling stage is not only affected directly by the fire HRR, but other factors such as the glowing embers and the residual heat in the enclosure boundaries which also contribute to the resultant design fire temperatures of the compartment. It is worth noting that similar discrepancies were also identified through using a CFD model for the Veselí Travelling Fire Test, by Horová *et al.*[29].

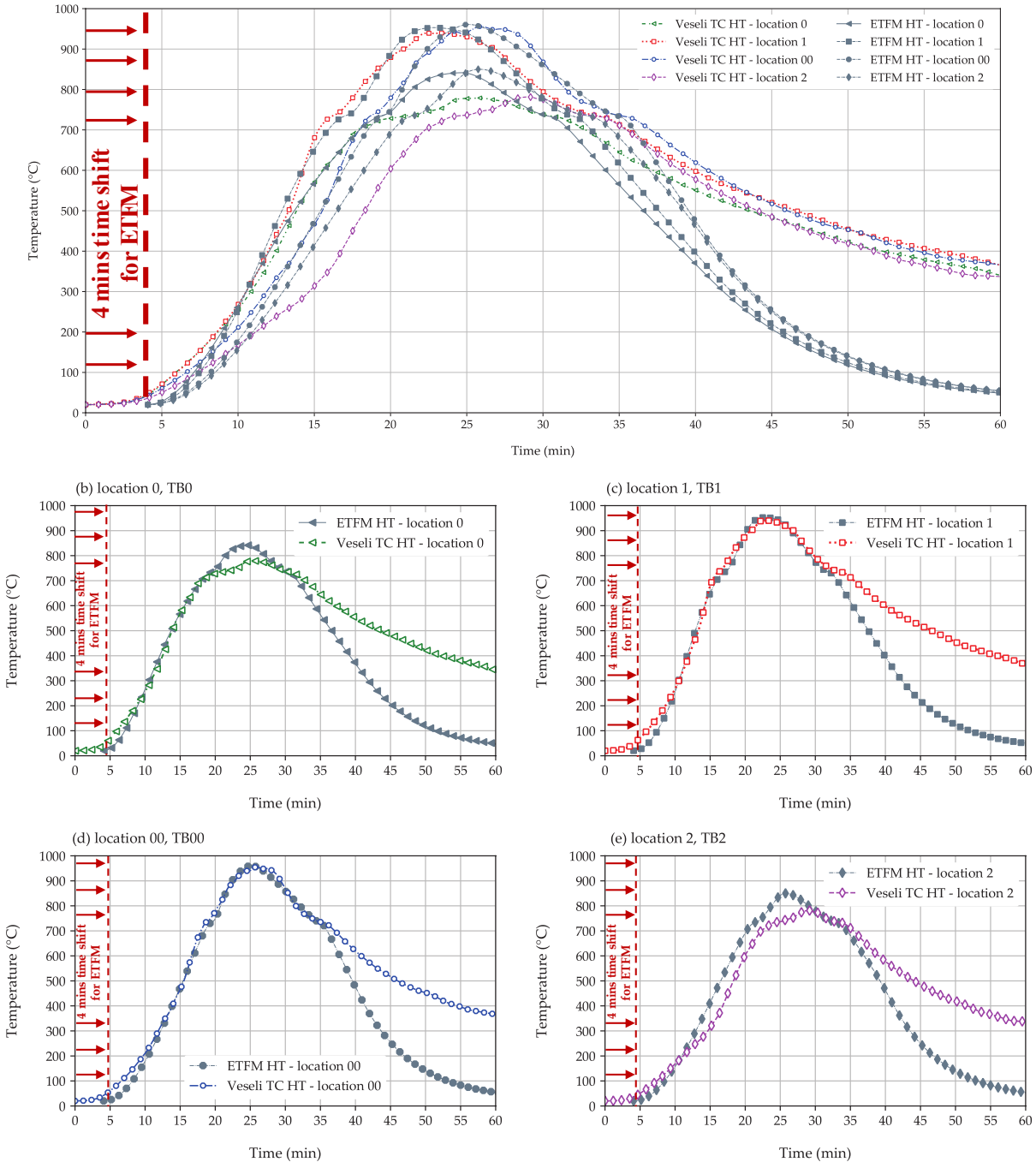

Figure 20. Comparison between the ETFM framework and the Veselí Test (with 4 mins time shift), using steel temperatures at bottom flanges, at various locations in the fire spread direction, (Veselí thermocouple (TC) temperatures at the vicinity of beam bottom flanges are used as input for SIFBuilder heat transfer (HT)), (a) all locations including 0, 1, 00 and 2, (b) location 0, (c) location 1, (d) location 00, and (e) location 2.

3.4 Parameter sensitivity studies on using the ETFM framework for VTFT

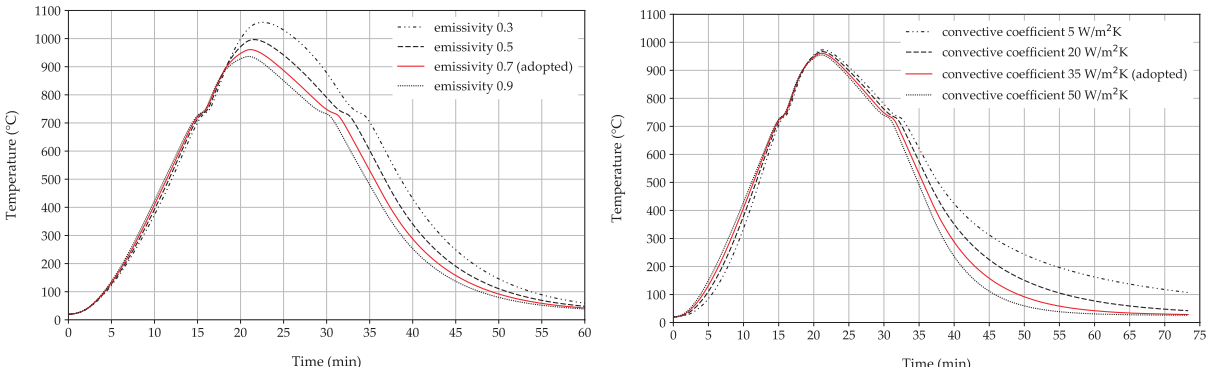

Figure 21. Steel beam bottom flange temperatures at location 00 using ETFM, with (a). various emissivity ε_m ranging from 0.3 to 0.9; (b). various convective coefficients h_c ranging from 5 W/m²K to 50 W/m²K.

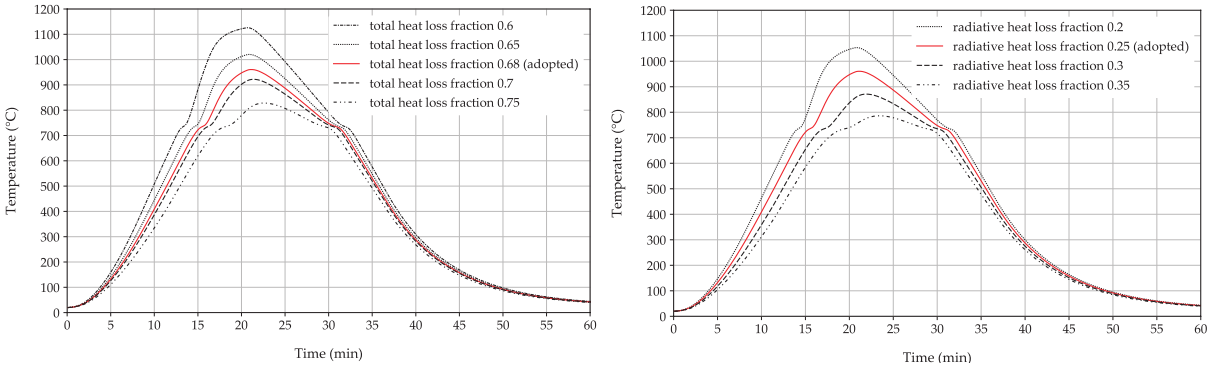

Figure 22. Steel beam bottom flange temperatures at location 00 using ETFM, with (a). various total heat loss fraction L_c ranging from 0.6 to 0.75; (b). various radiative heat loss fraction L_r ranging from 0.2 to 0.35.

To setup a travelling fire scenario using the ETFM framework in SIFBuilder under the Veselí travelling fire test case it is important to quantify the uncertainties of the input parameters, especially for the emissivity of the steel, ε_m, convective coefficient of the fire, h_c, total heat loss fraction, L_c, and radiative heat loss fraction, L_r. Figure 21(a) shows that ε_m affects the maximum temperatures that steel members can achieve, where higher $\varepsilon_m$values would generate lower steel temperatures. Figure 21(b) suggests the influence of h_c during the cooling phase of the travelling fire, where lower h_c values yield relatively higher steel member temperatures. This finding further suggests another source of the cooling stage temperature discrepancy found in Figure 20, that a constant $h_c = 35$ W/m² K is no longer realistic during the decaying stage of the fire. In such a case a lower h_c value may be more practical. Figure 22 suggests that both total heat loss fraction, L_c, and radiative heat loss fraction, L_r, dominate the maximum steel member temperatures, in which lower heat loss fraction values would generate lower resultant steel temperatures. It is worth noting that the uncertainties of those two heat loss fraction parameters, L_c and L_r, have fundamentally different origins: L_c is simply because of the complexity of the travelling fire processes, and in reality it is neither constant spatially or temporally, hence a lumped constant value was assumed in the FIRM zone model (see Eqns. 7 and 8), while L_r is a design parameter that is more related to the burning of fuel itself (see Janssens[19]). Nowadays, as buildings are tending to become more and more 'energy efficient', which means the energy loss is more limited and lower L_c values need to be addressed in design solutions.

4 Further Parametric Studies on using the ETFM Framework for VTFT

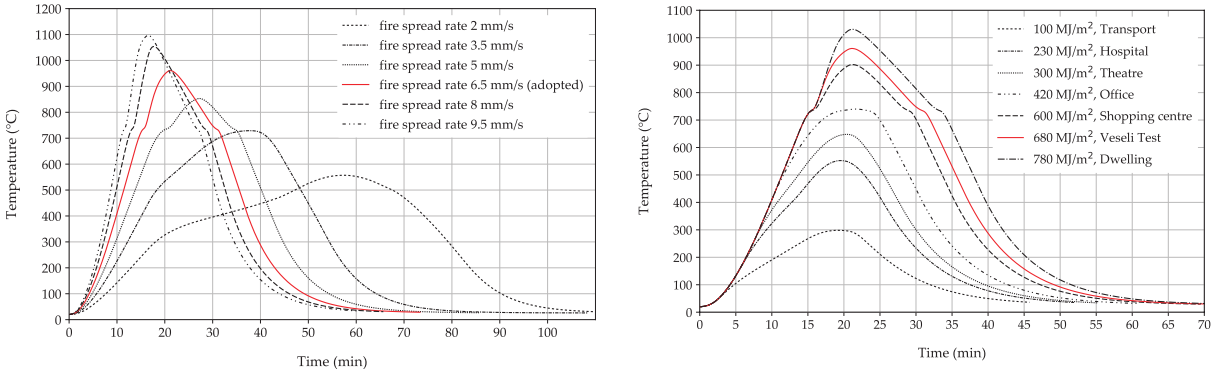

Figure 23. Steel beam bottom flange temperatures at location 00 using ETFM, with (a). various fire spread rates ranging from 2 mm/s to 9.5 mm/s; (b). various fuel load densities ranging from 100 MJ/m² to 780 MJ/m².

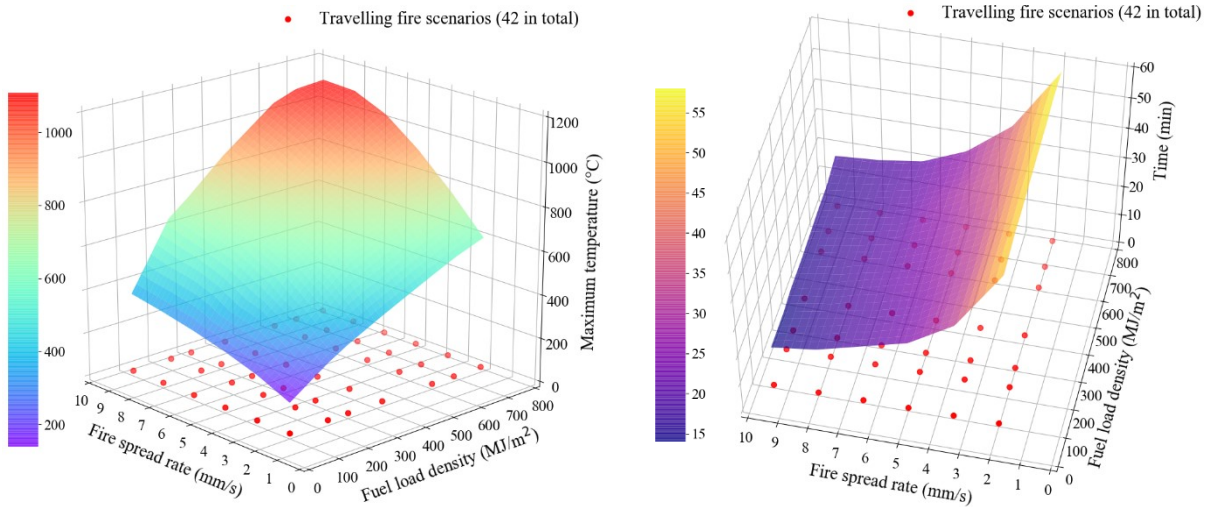

Figure 24. Various combinations of different fire spread rates (ranging from 2 mm/s to 9.5 mm/s) and fuel load densities (ranging from 100 MJ/m² to 780 MJ/m²) with 42 travelling fire scenarios, marked with red dots as sampling points, with (a). maximum steel beam bottom flange temperatures at location 00; (b). time to reach the peak temperature of the steel beam bottom flange at location 00.

When a structural engineer is to design a beam in a building, a design load must be chosen. The beam cannot be designed for all possible load combinations that would occur during the life of the structure. Hence, safety factors with specific building design loads are used for the engineer to make sure the member has enough 'load bearing margin' under different loading combinations. However, in structural fire design, there is no exact methodology or procedure available for the engineer to follow, especially while defining design fires within very large compartments, for performance-based design. Then it is recommended that the engineer should perform a series of design parametric analysis, through changing the design fire parameters to generate a family of travelling fires to check the reliability of their design solutions (e.g. including the maximum steel member temperatures, and the time to reach such temperatures). This section demonstrates such an effort. Following the same Veselí travelling fire test case, some of the design parameters are extended, such as various fuel load densities, opening dimensions, etc.

Figure 23(a) demonstrates that the travelling fire scenarios with higher fire spread rates, v (e.g. 8 mm/s, 9.5 mm/s) would generate higher temperatures and temperature increase rates. The reason is because, based on the energy conservation equation from the FIRM zone model, as presented in Eqn. 7, the resultant transient smoke layer temperature increases with higher HRR. The magnitude of HRR decides the amount of energy to be 'pumped' into the smoke layer at each time step. In addition, HRR is calculated based on the fire area in the ETFM framework, and fire area is a resultant of fire spread rate

and burning rate of the fuel (see Eqn. 12). Therefore, 'fast' fires produce higher thermal impact due to bigger fire areas and greater HRRs. Moreover, longer fire durations are generated when lower fire spread rates are used, such as the 2 and 3.5 mm/s travelling fires. Figure 23(b) shows that the travelling fire scenarios with higher fuel load densities generate higher steel temperatures. Again, it is also directly dependent on the HRR, which determines the amount of energy to be 'pumped' into the smoke layer at each time step, thus is dependent on the spread rate and burning rate. Larger fuel load densities would generate slower movement of the travelling fire trailing edge, thus a larger fire area would be produced. Therefore, 'dense' fires produce higher thermal impact due to bigger fire areas and HRR generated. In addition, Figure 23(b) also suggests that total fire durations are not sensitive to the variance of different fuel load densities.

Facilitated by ease of using the ETFM framework in SIFBuilder and its high computational efficiency, a large set of travelling fire scenarios combining various fire spread rates v and fuel load densities $q_{f,k}$ are further investigated, 42 in total. The values of v and $q_{f,k}$ are the same as the values presented in Figure 23(a) and (b) respectively, and further illustrated with corresponding red dots in Figure 24(a) and (b). Figure 24(a) demonstrates the maximum bottom flange temperatures of the investigated steel beam at location 00, ranging from 139 to 1108 °C. Higher maximum temperatures are captured with higher v and $q_{f,k}$, due to larger fire sizes and HRRs. Figure 24(a) implies v and $q_{f,k}$ are 'equally' influential on the resultant maximum temperatures, while for the travelling fire scenarios falling within the red ring (i.e. red: above 800 °C). However, such 'equivalent influence' diminishes while the travelling fire scenarios are stepping into the 'green and blue ring' (i.e. green and blue: below 800 °C). This green and blue ring changes its 'uniformity' compared with the red ring. It implies that the fuel load density has a stronger impact than fire spread rate under such fire scenario combinations. Figure 24(b) shows the time to reach maximum temperature of the investigated steel beam at location 00, ranging from 14 to 58 mins. This figure suggests that the fire spread rate is a more discriminating factor rather than the fuel load density, i.e. in terms of affecting time to reach peak temperatures in the beam.

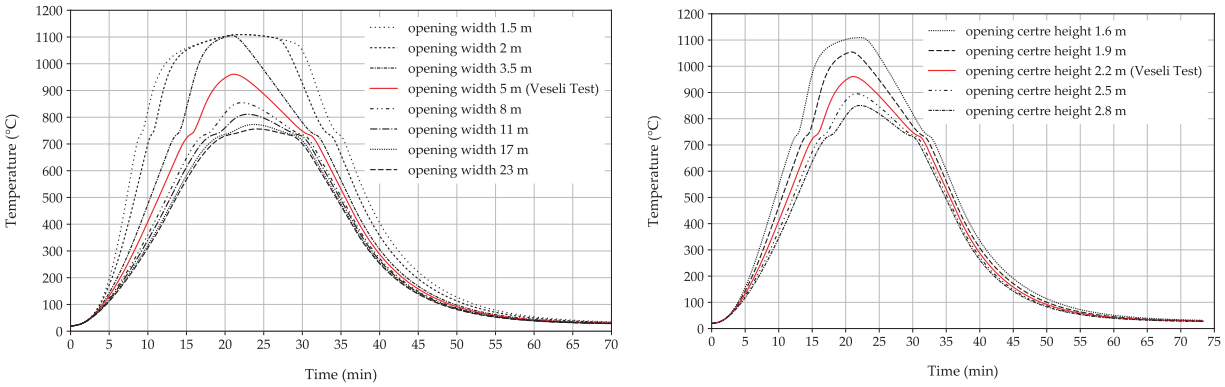

Figure 25. Steel beam bottom flange temperatures at location 00 using ETFM, with (a). various opening width W ranging from 1.5 m to 23 m; (b). various opening centre locations H_o, (sill height + soffit height)/2, ranging from 1.6 m to 2.8 m (opening dimension kept the same as the Veselí Travelling Fire Test Building, 5 m × 2 m).

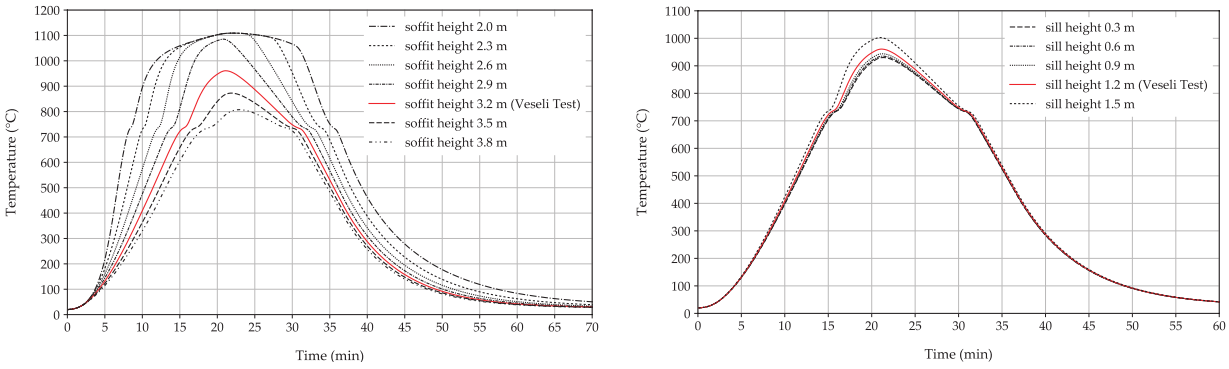

Figure 26. Steel beam bottom flange temperatures at location 00 using ETFM, with (a). various soffit heights ranging from 2.0 m to 3.8 m; (b). various sill heights ranging from 0.3 m to 1.5 m.

Figure 25(a) shows the impact of the opening width on the resultant steel member bottom flange time-temperature histories at location 00. It should be noted that all the input parameters for this series of travelling fires are the same as the ones presented in Figure 18, except for the variance of opening width. It suggests that smaller opening widths would yield higher steel temperatures and longer heating durations. The reason behind this observation is probably due to the fact that reducing the opening width will confine more upper smoke layer mass and energy within the compartment, i.e. less mass and energy from the hot upper layer is lost through the compartment openings, as suggested fundamentally by Eqns.6 and 7. It is worth noting that when the travelling fire scenarios have relatively small opening widths, i.e. 1.5, 2 and 3.5 m, then their maximum temperatures seem to coincide to an upper limit, approximately 1106 °C. This upper limit results from these small opening sizes, which constrain the ambient air inflow through the compartment cold layer, $(\dot{m}_a)_{max} = 0.52A_v\sqrt{H_v}$ (see section 2.2), for ventilation-controlled burning, while oxygen is limited. Figure 25(a) also further suggests that when the opening width is increasing to some extent, i.e. opening width is greater than 8 m in this Veselí case, that the dependence relationship between the maximum steel temperature and the opening width is not clear anymore. The maximum temperature of the steel member tends to be more related to the fuel load itself, rather than the openings. Figure 25(b) shows that the increase of the opening centre height would tend to decrease the steel member temperature, as the smoke hot layer neutral plane is 'moved upward', which reduces the stabilized smoke layer depth and corresponding hot temperature.

The influence of soffit height and sill height on the steel member bottom flange time-temperature history is presented in Figure 26(a) and Figure 26(b) respectively. Figure 26(a) suggests that increasing the height of the base of the soffit will generally bring down the steel member temperature. This is easy to understand, as the increased height corresponds to a reduced 'down-stand barrier' depth, which lowers the accumulated smoke layer depth and corresponding smoke layer temperature. Figure 26(b) implies that the sill height has very limited influence on the steel member time-temperature histories, unless this value reaches to 1.5 m, in this parametric study series. Further to the algorithm in the FIRM zone model regarding the sill height, this value is related to the calculation of the vent flow regimes and pressure difference for the neutral plane. The details of this calculation are not presented here due space, but can be found with full detail in Janssens[19].

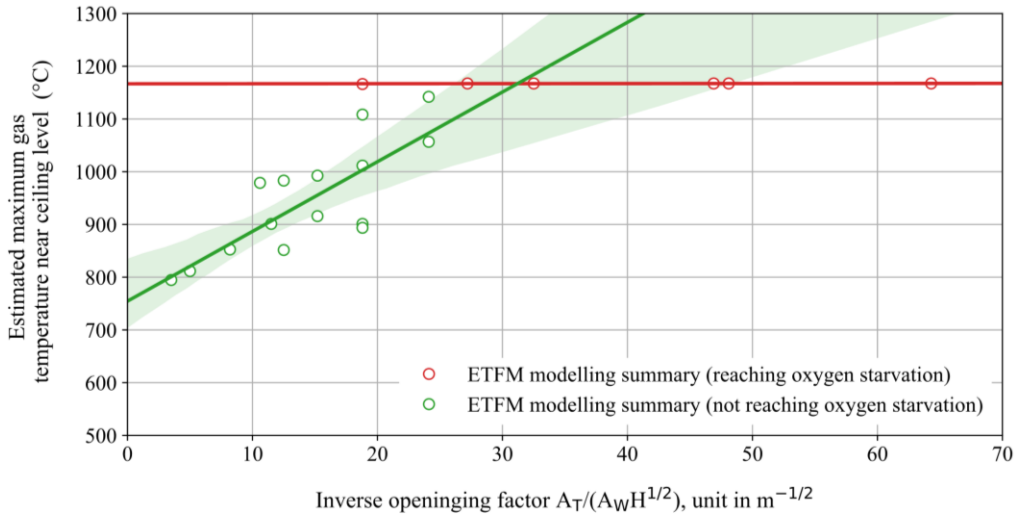

Figure 27. ETFM framework modelling summary of the parametric studies, data based on Figure 25 and Figure 26, in terms of inverse opening factors vs. estimated maximum gas temperatures near ceiling level (where A_T is the total area of enclosure excluding floor and openings, A_W is total area of vertical openings on all walls, and H is weighted average of window heights on all walls; the translucent band describes a bootstrap confidence interval of the estimated regression line according to the available data sampling points).

Figure 27 is a summary of the ETFM framework modelling results presented in Figure 25 and Figure 26, in terms of the corresponding inverse opening factors against the estimated maximum gas temperatures near ceiling level. This maximum temperature is estimated through dividing the relevant maximum steel member bottom flange temperature by 0.95. This relationship is a rough procedure for

estimating the unprotected steel member bottom flange temperature once the surrounding gas temperature is known, as suggested by a HERA (Heavy Engineering Research Association) report[61]. Unlike the ambiguity of the relationship between the compartment inverse opening factor and the measured maximum gas temperature near ceiling level (when the compartment inverse opening factor is less than 10, experimental review work shown in Figure 4), the green regression line in Figure 27 suggests that the modelling maximum travelling fire temperatures near the ceiling level scale with the increasing inverse opening factors. Once the inverse opening factors are large enough, a maximum temperature plateau is observed at around 1167 °C. This plateau arises because if the corresponding openings are relatively small compared with the whole compartment dimensions, then it forces the ETFM framework fire to step into the ventilation-controlled situation with 'oxygen starvation', triggering the ambient air inflow upper limit, i.e. $(\dot{m}_a)_{max} = 0.52A_v\sqrt{H_v}$. It is worth noting that this upper limit is a simplification for the modelling purpose, in reality the maximum temperatures will decrease as the inverse opening factors become very large, as suggested by Figure 4. Furthermore, Figure 27 suggest that the inverse opening factor with value of 30 divides the fuel-controlled regime and ventilation-controlled regime based on the ETFM framework modelling summary, this regime 'division number' apparently coincides with the same value of 30 as suggested by Figure 4 regarding the review work for large-scale travelling fire experiments.

5 Discussions on the Limitations of the ETFM Framework

This ETFM framework is developed for providing a more realistic tool for structural design of fire resistance in a large compartment. There are several inevitable limitations in the model. Firstly, it is essentially a 1D trajectory-based travelling fire model, which is currently strictly only applicable to floor plans with a core, or rectangular floorplan shape. Secondly, a potential limitation of the ETFM framework is the applicability of Hasemi's localized fire model, which is only strictly valid for fire diameters is less than 10m, and the rate of heat release less than 50MW[40], though these are very large fire sizes for typical compartments. Finally, the FIRM zone model is applicable for the ventilations with vertical openings through the walls, rather than horizontal openings through the ceiling, though the latter are much less common, and apply to scenarios with other complexities, e.g. basement fires. Furthermore, the venting is associated with natural ventilations, and forced ventilations are not considered[19].

Further to the above, the comparison between the ETFM framework and the Veselí test data shows that: 1) the current version of the ETFM framework uses a prescribed uniform fire spread rate, however in the test the fire spread rate is accelerating along the fire trajectory; 2) large discrepancies at the cooling stage of the travelling fire between the framework and the test are identified, meaning that the ETFM framework may overpredict the temperature decrease rate during the cooling stage of the travelling fire; this cooling temperature discrepancy is quite problematic, as the subsequent structural response analysis (e.g. using the finite element method) might be misinterpreted, i.e. exaggerated during the cooling stage of the fire; 3) uniform smoke layer assumption in the ETFM framework might be overly conservative for the structural elements at the far field; 4) though a good comparison in terms of the maximum steel temperatures and the relative timing of different steel member time-temperature histories along the travelling fire trajectory, it is worth noting that Veselí Travelling Fire Test is a single test which has its own limitations and simplifications; for example, the opening orientation is parallel to the fuel bed, which is a simpler case compared with the test series carried out by the BST/FRS[26] in 1993, in which the ventilation was confined to an opening at one end of the long compartment; in the latter test the fuel was ignited at the opposite end to the ventilation, and it was observed that the fire travelled quickly to the opening seeking air, then consumed all the fuel near the opening region, and finally travelled back to the ignition region as the fuel was progressively consumed. The ETFM framework cannot currently handle such scenarios.

In addition, according to the experimental review work in Figure 4 and the ETFM framework modelling summary in Figure 27, it has been shown that when the inverse opening factor becomes large (i.e. larger

than about 30), a maximum temperature plateau is employed in the ETFM through assuming an upper limit for the ambient air inflow. This is a conservative simplification compared to the reality found in Figure 4, where the maximum temperature will decrease as the inverse opening factor becomes very large.

6 Conclusions

A number of full-scale natural fire tests have been carried out in the large compartments where a clear travelling fire development had been identified or targeted. Investigation of the relationship between the inverse opening factor $A_T/(A_w H^{1/2})$ and the maximum average gas phase temperature $T_{g,max}$ near ceiling level suggests results which vary from classical observations in smaller compartments. Through comparing with the conventional regression curve for this relationship in small size compartments (< 150 m^3), it is found that the dependence of the relationship becomes weaker for large size compartments, especially for the cases under the fuel-controlled regime. Further, regime 'division number' apparently shifts from 10 for small size compartments to about 30 for large size compartments, which is first found in the experimental review work and seems to be supported by the subsequent ETFM framework modelling summary.

The full version of the ETFM framework with relevant design instructions, which can be readily used by the structural fire engineers, is presented in this paper. The ease of using the ETFM framework with a script, through a reliable computational tool SIFBuilder (covering fire modelling, heat transfer, and structural analysis), is also demonstrated.

Application of the ETFM framework to a real building, i.e. the Veselí Travelling Fire Test building, representing such a travelling fire scenario, is undertaken to further assess the capabilities and limitations of the framework. The comparison between the ETFM framework with the Veselí Travelling Fire Test confirms the capability of ETFM framework in predicting the maximum steel temperatures, and relative timing of different steel member time-temperature histories along the travelling fire trajectory. Those two capabilities are the most important elements for structural fire design under travelling fires, in the authors' opinion. Nevertheless, apart from the inherent limitations of the Hasemi's localised fire model and the FIRM zone model themselves, it is also identified that the uniform fire spread rate assumption, and underestimation of the temperatures during the cooling stage in the ETFM framework, are two important elements requiring to be improved in future work.

It is maintained that the inherent energy balance and mass balance from the FIRM zone model enable the ETFM framework to provide useful and practical insights on the thermal response with various parameters under more realistic fire scenarios (i.e. travelling fires) for performance-based design. The design parameter sensitivity studies, and parametric studies on the ETFM framework with the same Veselí Test Building case are carried out, to interprete the importance of different design parameters for travelling fires. It is found that fire spread rate and fuel load density are roughly equally determinative factors on the resultant maximum steel beam temperatures, while this value is higher than 800 °C for the Veselí Test Building case. However, such 'equivalent influence' diminishes while the travelling fire scenarios move into regimes resulting in lower resultant maximum temperatures, below 800 °C. This implies that the fuel load density has a slightly stronger impact than fire spread rate under such fire scenario combinations. Moreover, it also suggests that the fire spread rate is a more discriminating factor rather than the fuel load density, on affecting the time to reach the maximum beam temperatures. Furthermore, it has also been quantitatively demonstrated that the total heat loss fraction (e.g. through ceiling and wall linings) and the inverse opening factors are two important design parameters for travelling fires, which should be carefully selected for the design solutions. For example, choosing a small inverse opening factor (i.e. large openings compared with the entire compartment) for the design solution, would yield lower maximum steel member temperatures.

7 Acknowledgements

The authors would like to express their sincere thanks to Johan Sjöström who provided the access of the data for the TRAFIR-RISE Fire Test, David Rush who provided the access of the data for the Tisova Fire Test, and Juan P. Hidalgo who provided the access of the data for the Malveira Fire Test, for the review work of this paper. Frantisek Wald and Juan P. Hidalgo are gratefully acknowledged for their precious suggestions and discussions during the development of this work.

8 References

[1] Buchanan, A.H., and Abu, A.K. (2017). *Structural Design for Fire Safety*, Second Edi, Chichester, UK, John Wiley & Sons, Ltd.
[2] American Society for Testing and Materials. (2016). *Standard Test Methods for Fire Tests of Building Construction and Materials, ASTM E119.*, West Conshohocken, PA.
[3] Hasemi, Y., Yokobayashi, Y., Wakamatsu, T., and Ptchelintsev, A. V. (1996). Modelling of heating mechanism and thermal response of structural components exposed to localised fires, in: *Thirteenth Meeting of the UJNR Planel on Fire Research and Safety*. p. 237–247.
[4] Usmani, A.S., Chung, Y.C., and Torero, J.L. (2003). How did the WTC towers collapse: A new theory, *Fire Safety Journal*, 38(6), pp. 501–533.
[5] Gann, R.G., Hamins, A., McGrattan, K., Nelson, H.E., Ohlemiller, T.J., Prasad, K.R., and Pitts, W.M. (2013). Reconstruction of the fires and thermal environment in World Trade Center buildings 1, 2, and 7, *Fire Technology*, 49, pp. 679–707.
[6] Nelson, H.E. (1989). *An Engineering View of the Fire of May 4, 1988 in the First Interstate Bank Building, Los Angeles, California (NIST IR 89-4061)*, Gaithersburg, National Institute of Standards and Technology (NIST).
[7] Fletcher, I., Borg, A., Hitchen, N., and Welch, S. (2006). Performance of concrete in fire: A review of the state of the art, with a case study of the Windsor Tower fire, in: *4th International Workshop in Structures in Fire*. Aveiro, Portugal: Universidade de Aveiro, p. 779–790.
[8] Behnam, B. (2018). Fire structural response of the Plasco Building: A preliminary investigation report, *International Journal of Civil Engineering*, pp. 1–18.
[9] Yarlagadda, T., Hajiloo, H., Jiang, L., Green, M., and Usmani, A. (2018). Preliminary modelling of Plasco Tower collapse, *International Journal of High-Rise Buildings*, 7(4), pp. 397–408.
[10] Stern-Gottfried, J., and Rein, G. (2012). Travelling fires for structural design–Part I: Literature review, *Fire Safety Journal*, 54, pp. 74–85.
[11] Dai, X., Welch, S., and Usmani, A. (2017). A critical review of "travelling fire" scenarios for performance-based structural engineering, *Fire Safety Journal*, 91, pp. 568–578.
[12] Clifton, C.G. (1996). *Fire Models for Large Firecells. HERA Report R4-83*, HERA publications, New Zealand.
[13] Rein, G., Zhang, X., Williams, P., Hume, B., Heise, A., Jowsey, A., Lane, B., and Torero, J.L. (2007). Multi-storey fire analysis for high-rise buildings, in: *Proceedings of the 11th International Interflam Conference*. London, UK, p. 605–616.
[14] Stern-Gottfried, J., and Rein, G. (2012). Travelling fires for structural design-Part II: Design methodology, *Fire Safety Journal*, 54, pp. 96–112.
[15] Hopkin, D.J. (2013). Testing the single zone structural fire design hypothesis, in: *Proceedings of the 13th International Interflam Conference*. London, UK, p. 139–150.
[16] Rackauskaite, E., Hamel, C., Law, A., and Rein, G. (2015). Improved formulation of travelling fires and application to concrete and steel structures, *Structures*, 3, pp. 250–260.
[17] Dai, X., Jiang, L., Maclean, J., Welch, S., and Usmani, A. (2016). A conceptual framework for a design travelling fire for large compartments with fire resistant islands, in: *Proceedings of the 14th International Interflam Conference*. London, UK, p. 1039–1050.
[18] Dai, X., Jiang, L., Maclean, J., Welch, S., and Usmani, A. (2016). Implementation of a new design travelling fire model for global structural analysis, in: *The 9th International Conference on Structures in Fire*. Princeton, USA, p. 959–966.
[19] Janssens, M.L. (2000). *An Introduction to Mathematical Fire Modeling*, Second Edi, CRC Press.
[20] Drysdale, D. (2011). *An Introduction to Fire Dynamics*, Third Edit, Chichester, UK, A John Wiley & Sons, Ltd., Publication.
[21] Thomas, P.H., and Heselden, A.J. (1972). *Fully developed fires in single compartments, CIB Report No 20, Fire Research Note 923*, Borehamwood, England, UK.
[22] Torero, J.L., Majdalani, A.H., Abecassis-Empis, C., and Cowlard, A. (2014). Revisiting the compartment fire, in: *11th International Symposium on Fire Safety Science*. Christchurch, New-Zealand: International Association

for Fire Safety Science, p. 28–45.
[23] Majdalani, A.H., Cadena, J.E., Cowlard, A., Munoz, F., and Torero, J.L. (2016). Experimental characterisation of two fully-developed enclosure fire regimes, *Fire Safety Journal*, 79, pp. 10–19.
[24] Maluk, C., Linnan, B., Wong, A., Hidalgo, J.P., Torero, J.L., Abecassis-empis, C., and Cowlard, A. (2017). Energy distribution analysis in full-scale open floor plan enclosure fires, *Fire Safety Journal*, 91, pp. 422–431.
[25] Hidalgo, J.P., Cowlard, A., Abecassis-Empis, C., Maluk, C., Majdalani, A.H., Kahrmann, S., Hilditch, R., Krajcovic, M., and Torero, J.L. (2017). An experimental study of full-scale open floor plan enclosure fires, *Fire Safety Journal*, 89, pp. 22–40.
[26] Kirby, B.R., Wainman, D.E., Tomlinson, L.N., Kay, T.R., and Peacock, B.N. (1994). *Natural Fires in Large Scale Compartments*, British Steel Technical, Fire Research Station Collaborative Project Report, Rotherham, UK.
[27] British Steel plc, and Swinden Technology Centre. (1999). *The Behaviour of Multi-Storey Steel Framed Buildings in Fire (A European Joint Research Programme)*, Rotherham, UK.
[28] Moinuddin, K.A.M., and Thomas, I.R. (2009). An experimental study of fire development in deep enclosures and a new HRR–time–position model for a deep enclosure based on ventilation factor, *Fire and Materials*, 33, pp. 157–185.
[29] Horová, K., Jána, T., and Wald, F. (2013). Temperature heterogeneity during travelling fire on experimental building, *Advances in Engineering Software*, 62–63, pp. 119–130.
[30] Hidalgo, J.P., Cowlard, A., Abecassis-Empis, C., Maluk, C., Majdalani, A.H., Kahrmann, S., Hilditch, R., Krajcovic, M., and Torero, J.L. (2018). *Edinburgh Tall Building Fire Tests [dataset] (https://datashare.is.ed.ac.uk/handle/10283/3233)*, School of Engineering, University of Edinburgh.
[31] Goode, T. (2018). *Characterisation of the "Malveira Fire Test", Master Thesis*, The University of Queensland.
[32] Rush, D., and Lange, D. (2017). Towards a fragility assessment of a concrete column exposed to a real fire – Tisova Fire Test, *Engineering Structures*, 150, pp. 537–549.
[33] Gales, J. (2014). Travelling fires and the St. Lawrence Burns project, *Fire Technology*, 50(6), pp. 1535–1543.
[34] Hasemi, Y., and Tokunaga, T. (1984). Flame geometry effects on the buoyant plumes from turbulent diffusion flames, *Fire Science and Technology*, 4, pp. 15–26.
[35] Hasemi, Y., Yokobayashi, Y., Wakamatsu, T., and Ptchelintsev, A. (1995). Fire safety of building components exposed to a localized fire - scope and experiments on ceiling beam system exposed to a localized fire, in: *ASIAFLAM's 95, Hong Kong*. Hong Kong.
[36] Pchelintsev, A., Hasemi, Y., Wakamatsu, T., and Yokobayashi, Y. (1997). Experimental and numerical study on the behaviour of a steel beam under ceiling exposed to a localized fire, in: *Fire Safety Science - Proceedings of the 5th International Symposium*. p. 1153–1164.
[37] Wakamatsu, T., Hasemi, Y., and Ptchelintsev, A. V. (1997). Heating mechanism of building components exposed to a localized fire - FDM thermal analysis of a steel beam under ceiling, in: *Proceedings of the 1997 16th International Conference on Offshore Mechanics and Arctic Engineering*. Yokohama, Japan: ASME, p. 51–58.
[38] Kruppa, J., Joyeux, D., and Zhao, B. (2005). Scientific background to the harmonization of structural Eurocodes, *HERON*, 50(4), pp. 219–235.
[39] Commission of the European Community (CEC) (1997b). (1997). *Development of Design Rules for Steel Structures Subjected to Natural Fires in Closed Car Parks*.
[40] CEN European Standard EN 1991-1-2. (2002). *Eurocode1: Actions on Structures - Part 1-2: General Actions - Actions on Structures Exposed to Fire*, Brussels.
[41] Cadorin, J.-F., and Franssen, J.-M. (2003). A tool to design steel elements submitted to compartment fires—OZone V2. Part 1: pre- and post-flashover compartment fire model, *Fire Safety Journal*, 38(5), pp. 395–427.
[42] Cadorin, J.-F., Pintea, D., Dotreppe, J.-C., and Franssen, J.-M. (2003). A tool to design steel elements submitted to compartment fires—OZone V2. Part 2: Methodology and application, *Fire Safety Journal*, 38(5), pp. 429–451.
[43] Peacock, R.D., Mcgrattan, K.B., Forney, G.P., and Reneke, P.A. (2017). *CFAST – Consolidated Fire and Smoke Transport (Version 7) Volume 1 : Technical Reference Guide*, National Institute of Standards and Technology.
[44] American Society for Testing and Materials. (2004). *ASTM E1355-04, Standard Guide for Evaluating the Predictive Capabilities of Deterministic Fire Models*, West Conshohocken, Pennsylvania.
[45] Kumar, S., Chitty, R., and Welch, S. (2003). Development and validation of integrated fire modelling methodology for smoke ventilation design and hazard assessment in large buildings, in: *Proceedings of the 4th International Seminar on Fire & Explosion Hazards*. p. 629–641.
[46] Thomas, P.H., Hinkley, P.L., and Theobald, C.R. (1963). *Investigations into the Flow of Hot Gases in Roof Venting*, BRE Archive.
[47] Zukoski, E.E., Kubota, T., and Cetegen, B. (1981). Entrainment in fire plumes, *Fire Safety Journal*, 3(3), pp. 107–121.
[48] Buchanan, A. (2008). The challenges of predicting structural performance in fires, in: *Fire Safety Science – Proceedings of the Ninth International Symposium*. p. 79–90.

[49] Commission of the European Community (CEC) (1997a). (1997). *Development of Design Rules for Steel Structures Subjected to Natural Fires in Large Compartments*.
[50] Babrauskas, V. (1998). Glass breakage in fires, *The Fire Place, Washington Chapter IAAI Newsletter*, pp. 15–17.
[51] McKenna, F.T. (1997). *Object-Oriented Finite Element Programming: Frameworks for Analysis, Algorithms and Parallel Computing*, PhD Thesis, the University of California.
[52] Dai, X., Jiang, Y., Jiang, L., Welch, S., and Usmani, A.S. (2017). Implementation of fire models in OpenSees, in: *Proceedings of the 1st European Conference on OpenSees*. Porto, Portugal: Faculty of Engineering, University of Porto, p. 47–50.
[53] Dai, X. (2017). *An extended travelling fire method framework with an OpenSees-based integrated tool SIFBuilder*, PhD Thesis, The University of Edinburgh.
[54] Simões da Silva et al., L. (2014). *Design of Composite Joints for Improved Fire Robustness, RFCS Compfire project-final report (RFSR-CT-2009-00021)*, Luxembourg.
[55] Wald, F., Jána, T., and Horová, K. (2011). *Design of Joints to Composite Columns for Improved Fire Robustness: To Demonstration Fire Tests*, Czech Technical University in Prague.
[56] Horová, K. (2015). *Modelling of Fire Spread in Structural Fire Engineering*, PhD Thesis, Czech Technical University in Prague.
[57] Karlsson, B., and Quintiere, J.G. (1999). *Enclosure Fire Dynamics*, 1st Edi, CRC Press.
[58] Jiang, Y. (2012). *Development and Application of a Thermal Analysis Framework in OpenSees for Structures in fire*, PhD Thesis, the University of Edinburgh.
[59] Welch, S., Jowsey, A., Deeny, S., Morgan, R., and Torero, J.L. (2007). BRE large compartment fire tests-Characterising post-flashover fires for model validation, *Fire Safety Journal*, 42(8), pp. 548–567.
[60] Torero, J.L. (2013). Scaling-Up fire, *Proceedings of the Combustion Institute*, 34, pp. 99–124.
[61] HERA. (2006). *Steel Structures Seminar: Earthquake, Wind and Fire, HERA Report R4-139*, Manukau City, New Zealand, New Zealand Heavy Engineering Research Association.
[62] Welch, B.B., Jones, K., and Hobbs, J. (2003). *Practical Programming in Tcl and TK*, 4th Ed, Prentice Hall.